Non-Markovianity in atom-surface dispersion forces

F. Intravaia, R. O. Behunin, C. Henkel, K. Busch, and D. A. R. Dalvit

Phys. Rev. A **94**, 042114 — Published 18 October 2016

DOI: 10.1103/PhysRevA.94.042114

Non-Markovianity in atom-surface dispersion forces

F. Intravaia,[1] R. O. Behunin,[2] C. Henkel,[3] K. Busch,[1,4] and D. A. R. Dalvit[5]

[1] *Max-Born-Institut, 12489 Berlin, Germany*
[2] *Department of Applied Physics, Yale University, New Haven, Connecticut 06511, USA*
[3] *Institute of Physics and Astronomy, University of Potsdam, Karl-Liebknecht-Str. 24/25, 14476 Potsdam, Germany*
[4] *Humboldt-Universität zu Berlin, Institut für Physik, AG Theoretische Optik & Photonik, 12489 Berlin, Germany*
[5] *Theoretical Division, MS B213, Los Alamos National Laboratory, Los Alamos, NM 87545, USA*

We discuss the failure of the Markov approximation in the description of atom-surface fluctuation-induced interactions, both in equilibrium (Casimir-Polder forces) and out-of-equilibrium (quantum friction). Using general theoretical arguments, we show that the Markov approximation can lead to erroneous predictions of such phenomena with regard to both strength and functional dependencies on system parameters. In particular, we show that the long-time power-law tails of temporal correlations, and the corresponding low-frequency behavior, of two-time dipole correlations, neglected in the Markovian limit, affect the prediction of the force. Our findings highlight the importance of non-Markovian effects in dispersion interactions.

PACS numbers: 42.50.Ct, 12.20.-m, 78.20.Ci

I. INTRODUCTION

Prototypical examples of dispersion interactions mediated by the quantum electromagnetic field are the Casimir-Polder force on a static atom close to a surface [1], and the quantum frictional force experienced by the same atom as soon as it starts moving above the surface [2, 3]. From a theoretical standpoint, one must often rely on approximations to model such interactions and predict the outcome of a specific experimental setup. One of these is the Markov approximation, which is also one of the most ubiquitous and successful approximations used in quantum optics and has provided reliable predictions for numerous experimental setups. In Casimir physics, the Markov approximation can be employed to simplify the equations describing the coupled atom-surface-radiation dynamics, making them solvable. The key assumption underlying this approximation is that the system's memory can be ignored, i.e., the future of its dynamics is only related to the immediate present. More specifically, the logic behind this approach finds its justification in the fact that sub-systems often exhibit very different correlation times, so that on average the fastest dynamics blurs the evolution of the slower sub-system, effectively erasing its memory [4, 5]. Usually, Markovian dynamics results in exponential decays of observables, while non-Markovian effects lead to more complex behaviors (see Sec. II B below). This simple difference has been used to discriminate between these two regimes [6, 7]. While in recent years more precise measures of non-Markovianity in quantum systems have been suggested [6–9], we focus in this work, for simplicity, on deviations from exponential behavior.

A key result of this paper is that the Markov approximation fails to provide reliable predictions for non-equilibrium fluctuation-induced interactions. Surprisingly, depending on the targeted level of accuracy, it can lead to incorrect results for systems in equilibrium. Although in some circumstances non-Markovian effects are known to strongly affect the dynamics of quantum systems (e.g. non-exponential decay of excited quantum states for atoms in photonic crystals [10]), their impact on fluctuation-induced phenomena in and out of equilibrium has not been thoroughly explored. Our discussion focuses on the prototypical system consisting of a single atom (or, in general, a microscopic system with internal degrees of freedom) interacting with a planar surface (see Figs. 1 and 4). Besides the large interest of modern experiments in such setups [11], e.g., in infrared near-field microscopy and hybrid atom-chip systems, these examples lend themselves to advanced but still not too complex theoretical treatments.

Our paper is organized as follows. In Section II we review the theory of equilibrium atom-surface interactions and derive the expression for the Casimir-Polder force (see Fig. 1). The purpose of this part is twofold: On the one hand, it allows for an exposition of the formalism and the basic concepts which will be used in the non-equilibrium case. On the other hand, our approach allows for considerations beyond standard perturbative techniques [11, 12] and the usual Lifshitz theory of equilibrium phenomena [13]. In particular, we show that long-time tails in the two-time dipole correlation (and its corresponding low-frequency behavior) arising from non-Markovian effects become relevant as soon as one goes beyond second-order perturbation theory (see Fig. 3). Since Casimir interactions are a broad-band frequency phenomenon, a precise description of the behavior at all frequencies is important for the evaluation of the interaction. Our final result will formally take into account the general response of the atomic system, and the standard Lifshitz formula is obtained as a special case.

Section III focuses on quantum friction. Like ordinary friction, this effect describes a force acting on an object

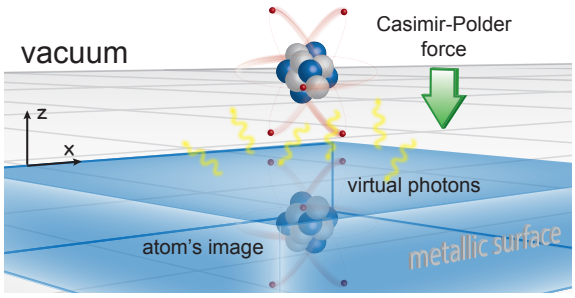

FIG. 1: Schematic of an atom above a surface experiencing the Casimir-Polder force. The presence of the correlation tensor in the expression of the force Eq.(4) can be qualitatively understood as stemming from the interaction of the atom with its image within the material.

moving near another one (see Fig. 4). Unlike the classical case, however, quantum friction is mediated by the interaction with the electromagnetic field at zero temperature. We argue that, as for an atom at rest, non-Markovian effects influencing the low-frequency behavior of the dipole correlator are crucial for the correct evaluation of this drag force, in particular its velocity dependency (see Eqs. (28) and (29) below). In Section IV we discuss quantum friction within lowest-order perturbation theory, and analyze the impact of intrinsic or induced dissipation on the drag force. Finally, Section V contains a brief summary and discussion of the key results of this work.

II. NON-MARKOVIAN EFFECTS WITHIN THE CASIMIR-POLDER INTERACTION

Let us start by considering the familiar Casimir-Polder interaction between an atom located at position $\mathbf{r}_a$ above a semi-infinite planar medium (see Fig. 1). In our description, the atom is represented by the dipole operator $\hat{\mathbf{d}}(t)$. For symmetry reasons, the force acting on the atom is oriented normal to the planar interface (which we denote as the z-direction). At any given time t, it is given by

$$F_{\rm CP}(t) = \langle \hat{\mathbf{d}}(t) \cdot \partial_{z_a} \hat{\mathbf{E}}(\mathbf{r}_a, t) \rangle, \tag{1}$$

where $\hat{\mathbf{E}}(\mathbf{r}, t)$ is the electric field operator. This expression for the atom-surface force can be derived from the Lorentz force on the atom [12]. It is important to stress that the time dependence of the operators in Eq.(1) is the full time evolution dictated by the total system and, therefore, it includes the effect of the interactions between the different subsystems (atom, field, and matter).

Using the Maxwell equations, the electric field operator can be written as $\hat{\mathbf{E}}(\mathbf{r}, t) = \hat{\mathbf{E}}^{(+)}(\mathbf{r}, t) + \text{h.c.}$, where

$$\hat{\mathbf{E}}^{(+)}(\mathbf{r}, t) = \hat{\mathbf{E}}_0^{(+)}(\mathbf{r}, t) + \frac{\mathrm{i}}{\pi} \int_0^\infty d\omega \int_{t_i}^t dt' e^{-\mathrm{i}\omega(t-t')} \underline{G}_I(\mathbf{r}, \mathbf{r}_a, \omega) \cdot \hat{\mathbf{d}}(t'), \tag{2}$$

with t_i being some initial time. Here, $\hat{\mathbf{E}}_0^{(+)}$ is the positive-frequency part (related to the annihilation operators) of the electromagnetic field in the absence of the atom but in the presence of the dissipative medium, and $\underline{G}(\mathbf{r}, \mathbf{r}', \omega)$ is the Green tensor of the half-space associated with the surface. To derive equation (2) we used the Kramers-Kronig relations for the Green tensor (see Appendix A). Hereafter we adopt the subscripts "I" and "R" to, respectively, indicate the imaginary and the real part of a quantity (component-wise for tensorial objects). Because the dipole and the field (positive- and negative-frequency parts separately) operators commute at equal times, by normal ordering we can write

$$\begin{aligned} F_{\rm CP}(t) &= \langle \hat{\mathbf{d}}(t) \cdot \partial_{z_a} \hat{\mathbf{E}}^{(+)}(\mathbf{r}_a, t) \rangle + \text{h.c.} \\ &= 2\mathrm{Re} \langle \hat{\mathbf{d}}(t) \cdot \partial_{z_a} \hat{\mathbf{E}}^{(+)}(\mathbf{r}_a, t) \rangle. \end{aligned} \tag{3}$$

The final result cannot depend on the ordering we choose, as long as this ordering is consistently used throughout the entire derivation. However, as will appear in the following, this specific choice of ordering is convenient for our calculations. Physically it has the implication of attributing the force exclusively to the radiation reaction in the atom dynamics [14], while the contribution of the vacuum field related to the operator $\hat{\mathbf{E}}_0$ seemingly disappears. However, this does not mean that the quantum properties $\hat{\mathbf{E}}_0$ are irrelevant: In this approach they are "hidden" in the expression for the time-dependent dipole operator and they will explicitly appear again when we consider, for example, dipole correlation functions. For other choices, such as symmetric ordering [15], both the dipole and the field itself contribute to the force and the term containing $\hat{\mathbf{E}}_0$ must consistently be kept throughout the calculation.

To evaluate the force, let us assume an initially factorized state $\hat{\rho}(t_i) = \hat{\rho}_a(t_i) \bigotimes \hat{\rho}_{\rm f/m}(t_i)$, where $\hat{\rho}_a(t_i)$ is the atom's initial density matrix and $\hat{\rho}_{\rm f/m}(t_i)$ represents the state of the coupled field/matter system. Both subsystems are assumed to be initially in their respective ground states, which implies that $\langle \hat{\mathbf{d}}(t) \cdot \partial_{z_a} \hat{\mathbf{E}}_0^{(+)}(\mathbf{r}_a, t) \rangle = \mathrm{tr}[\hat{\mathbf{d}}(t) \cdot \partial_{z_a} \hat{\mathbf{E}}_0^{(+)}(\mathbf{r}_a, t) \hat{\rho}(t_i)] = 0$ for all times (here, the symbol "tr" traces over the quantum states). This means that the contribution coming from the vacuum state of field plus medium subsystem drops out of the calculation. Note that, although both subsystems are initially in their respective ground states, in general, the state $\hat{\rho}(t_i)$ *is not* the ground state of the composite system [16, 17]. During the course of the time-evolution, the atom subsystem becomes entangled with the field/matter subsystem, undergoing the well-known "dressing" process [18].

Using the decomposition in Eq. (2) and the symmetry properties of the Green tensor, $G_{ij}(\mathbf{r}, \mathbf{r}', \omega) = G_{ji}(\mathbf{r}', \mathbf{r}, \omega)$ (we consider only reciprocal media), we can

rewrite the atom-surface force as

$$F_{\rm CP}(t) = {\rm Re}\Bigg(\frac{2{\rm i}}{\pi} \int_0^\infty d\omega \int_0^{t-t_i} d\tau e^{-{\rm i}\omega\tau} \times {\rm Tr}\left[\underline{C}(t, t-\tau) \cdot \partial_z \underline{G}_I(\mathbf{r}_a, \mathbf{r}, \omega)_{|\mathbf{r}=\mathbf{r}_a} \right] \Bigg), \quad (4)$$

where "Tr" traces over tensor indices and we have set $\tau = t - t' > 0$. The tensor $\underline{C}$ is the (non-symmetrically ordered) two-time dipole correlator,

$$C_{ij}(t, t-\tau) = \langle \hat{d}_i(t) \hat{d}_j(t-\tau) \rangle, \quad (5)$$

which plays a key role in what follows. Although it is in general highly non-trivial, the coupled equations of motion for the atom and field/matter can be solved (e.g. numerically or using the Born-Markov approximation [12]) to obtain the dynamic evolution of the two-time dipole correlator and the time-dependent atom-surface force.

A natural question that arises is whether non-Markovian effects are relevant in the dynamics of the dipole correlator and, consequently, in the force $F_{\rm CP}(t)$. In order to address this question, we will consider the limit of large times in which the entire system of atom plus field/matter evolves to a stationary state. In this case, the correlator depends only on the time difference τ, i.e., $C_{ij}(t, t-\tau) \to C_{ij}(\tau) = {\rm tr}[\hat{d}_i(\tau)\hat{d}_j(0)\hat{\rho}(\infty)]$, where $\hat{\rho}(\infty)$ represents the stationary density matrix of the full system. In this limit the atom-surface force reaches the constant value $F_{\rm CP} \equiv \lim_{t\to\infty} F_{\rm CP}(t)$, which should coincide with the expression of the well-known Casimir-Polder interaction [1]. In order to evaluate Eq.(4) for large times, it is convenient to introduce the dipole power spectrum tensor $\underline{S}(\omega)$, which is defined in terms of the correlator as

$$\underline{S}(\omega) = \frac{1}{2\pi} \int_{-\infty}^{\infty} d\tau e^{{\rm i}\omega\tau} \underline{C}(\tau). \quad (6)$$

As $\underline{C}^\dagger(\tau) = \underline{C}(-\tau)$, the power spectrum is Hermitian $\underline{S}^\dagger(\omega) = \underline{S}(\omega)$ and its real part $\underline{S}_R(\omega)$ is a symmetric matrix, while its imaginary part $\underline{S}_I(\omega)$ is anti-symmetric. Using these properties, the stationary Casimir-Polder force can be written as

$$F_{\rm CP} = \frac{2}{\pi} \int_0^\infty d\omega \int_{-\infty}^{\infty} d\nu \times {\rm P}\left(\frac{{\rm Tr}\left[\underline{S}_R(\nu) \cdot \partial_z \underline{G}_I(\mathbf{r}_a, \mathbf{r}, \omega)_{|\mathbf{r}=\mathbf{r}_a} \right]}{\omega + \nu} \right), \quad (7)$$

where P denotes the principal value and we have used that the matrix $\partial_z \underline{G}_I(\mathbf{r}_a, \mathbf{r}, \omega)_{|\mathbf{r}=\mathbf{r}_a}$ is symmetric (see Appendix A), and trace-orthogonal to any anti-symmetric matrix.

As we will show below, depending on the approach and the approximations used to compute this stationary dipole-dipole power spectrum, one obtains different expressions for the stationary Casimir-Polder interaction.

A. Using the fluctuation-dissipation theorem

At large times one can invoke equilibrium considerations to determine the stationary density matrix. We assume that the full system thermally equilibrates to a Gibbs state [5, 19–21] and appeal to the fluctuation-dissipation theorem (FDT) [22]. This theorem of equilibrium thermodynamics establishes a connection between the power spectrum and the linear response of the system to a small external perturbation. At zero temperature ($T = 0$) and for a non-symmetrized correlator, the FDT takes the form [20]

$$\underline{S}(\omega) = \frac{\hbar}{\pi} \theta(\omega) \underline{\alpha}_{\Im}(\omega), \quad (8)$$

where $\theta(\omega)$ denotes the Heaviside function, and $\underline{\alpha}_{\Im}(\omega) = [\underline{\alpha}(\omega) - \underline{\alpha}^\dagger(\omega)]/(2{\rm i}) = \underline{\alpha}^{\rm s}_I(\omega) - {\rm i}\underline{\alpha}^{\rm as}_R(\omega)$ (the superscripts "s" and "as" indicate the symmetric and the anti-symmetric part of the tensor). Further, $\underline{\alpha}(\omega)$ represents the atom's complex susceptibility (polarizability) tensor, i.e. the Fourier transform of Kubo's formula in the case of linear response, i.e.,

$$\alpha_{ij}(\tau) = \frac{\rm i}{\hbar} \theta(\tau) {\rm tr}\{[\hat{d}_i(\tau), \hat{d}_j(0)]\hat{\rho}(\infty)\}. \quad (9)$$

As any susceptibility (including the Green tensor), $\underline{\alpha}(\omega)$ is analytic in the upper part of the complex ω-plane and satisfies the crossing relation $\underline{\alpha}(-\omega^*) = \underline{\alpha}^*(\omega)$. It follows that the real (imaginary) part of the polarizability is an even (odd) function of frequency. Using these properties in combination with the FDT and the Kramers-Kronig relations, and following a procedure similar to that of Ref. [23], we may rewrite Eq.(7) as

$$F_{\rm CP} = \frac{\hbar}{\pi} \int_0^\infty d\xi \, {\rm Tr}\left[\underline{\alpha}({\rm i}\xi, \mathbf{r}_a) \cdot \partial_z \underline{G}(\mathbf{r}_a, \mathbf{r}, {\rm i}\xi)_{|\mathbf{r}=\mathbf{r}_a} \right] . \quad (10)$$

Here, we exploited the analytic properties of $\underline{\alpha}(\omega, \mathbf{r})$ and $\underline{G}(\mathbf{r}, \mathbf{r}', \omega)$ in the complex ω plane to express the final result as an integral along the positive imaginary-frequency axis (Wick rotation). In the above expression, we have explicitly indicated the position dependence of the atom's polarizability to stress that the dressing is depending on the system's geometry. Notice that because of the symmetries of the Green tensor, only the symmetric part of the polarizability, $\underline{\alpha}^{\rm s}(\omega, \mathbf{r})$, is relevant in Eq. (10).

As a final remark of this subsection, we want to emphasize that, despite certain formal similarities, Eq. (10) differs from standard formulas found in the literature for the atom-surface dispersive interaction. Indeed, Eq. (10) contains the exact atomic polarizability, while standard expressions are special cases of this formula, e.g. the Lifshitz formula for linear systems [13], and perturbative expansions in the atom-field coupling strength [1, 23, 24]. For further details, see Appendix B.

B. Using the quantum regression theorem

In quantum optics, one of the most widely used tools to evaluate two-time correlators is the quantum regression theorem (QRT) [12, 25, 26]. Often considered as the quantum extension of Onsager's regression conjecture [27, 28], the QRT finds its justification within the framework of master equations. Using the Born approximation, it is possible to show that the equations of motion for the correlations are the same as those for the mean values [25].

Mathematically, this can be formulated in the following terms. Given a generic subsystem coupled to a stationary environment, by using only the Born approximation one can write (see Appendix C)

$$\partial_\tau C_B^{nm}(t,\tau) = \sum_{ij} \left[-\mathrm{i}\omega_{ij}\delta_{ij}^{nm} - \mathcal{L}_{ij}^{nm}(\tau)\right] C_B^{ij}(t,\tau). \quad (11)$$

Here $C_B^{nm}(t,\tau) = \mathrm{Tr}[\hat{A}_{mn}(t+\tau)\hat{B}(t)\rho(0)]$ ($\tau > 0$) with $\hat{B}$ a generic operator and $\hat{A}_{mn} = |E_m\rangle\langle E_n|$, where $|E_n\rangle$ is an eigenvector the of the subsystem's (isolated) Hamiltonian. In addition we have defined $\omega_{ij} = (E_i - E_j)/\hbar$, $\delta_{ij}^{nm} = \delta_{ni}\delta_{mj}$, and $\mathcal{L}_{ij}^{nm}(\tau) = \mathrm{Tr}_S[\hat{A}_{nm}^\dagger \mathcal{L}(\tau)\hat{A}_{ij}]$ where $\mathcal{L}(\tau)$ is the Liouvillian describing the subsystem's reduced dynamics stemming from the interaction with the environment [4, 5]. Depending on the chosen approach this superoperator is either a functional describing the convolution with a kernel function (time non-locality) or an infinite series involving the generalized cumulants of the interaction Hamiltonian [4, 5]. If $\hat{B}$ is the identity Eq. (11) describes the evolution of the mean value of $\hat{A}_{mn}$. For $\hat{B} = \hat{A}_{n'm'}$, the same equation describes the evolution of the correlation $\langle \hat{A}_{mn}(t+\tau)\hat{A}_{n'm'}(t)\rangle$.

Usually, the equations of motion (11) can only be solved by using the Markov approximation (time local approach, no memory effects). In this approximation $\mathcal{L}_{ij}^{nm}(\tau)$ becomes a constant number, and Eq. (11) takes the form $\partial_\tau C_B^{nm}(t,\tau) = -\sum_{ij} \mathcal{M}_{ij}^{nm} C_B^{ij}(t,\tau)$, which can be solved by diagonalizing the matrix $\mathcal{M}_{ij}^{nm}$. The solution can be expressed as a sum of exponentials $\exp[-(\mathrm{i}\tilde{\omega}_\mu + \gamma_\mu)\tau]$, where $\tilde{\omega}_\mu$ and $\gamma_\mu > 0$ are the shifted transition frequencies (related to ω_{nm}) and decay rates induced by the environment [4, 5, 29]. In the usual master equation framework it is expected that, in the absence of any external driving force and at large times, the reduced density matrix of the subsystem should relax to its equilibrium state [5, 12]. In particular, at zero temperature this reduced density matrix should relax to the subsystem's ground state and therefore $\langle \hat{A}_{mm'}(t\to\infty)\rangle = \delta_{mg}\delta_{m'g}$ [30]. Although the QRT provides expressions for correlators that are often more explicit than those in the FDT, the approximations on which it relies limit its validity to the limit of weak coupling and to a narrow range of frequencies close to a resonance [31–35].

To show how this affects the Casimir-Polder interaction, we now evaluate the two-time dipole correlation tensor introduced at the beginning of this section using the Born-Markov approximation and the QRT approach. For simplicity, let us model the atom as a two-state system (ground state $|g\rangle$, excited state $|e\rangle$) and introduce the transition operator $\hat{A}_{ge} = |g\rangle\langle e|$ and its conjugate. We write the dipole operator as $\hat{\mathbf{d}}(t) = \mathbf{d}(|g\rangle\langle e| + |e\rangle\langle g|)$, where $\mathbf{d}$ denotes the (real) dipole vector [36, 37]. (Similar results can be obtained by modeling the dipole operator in terms of a harmonic oscillator.) According to the QRT, the stationary ($t\to\infty$) two-time correlation tensor $\underline{C}(\tau)$ (Eq. (5)) evolves as a single exponential [5, 12, 26]

$$C_{ij}(\tau) = d_i d_j\, e^{-\mathrm{i}\tilde{\omega}_a(\mathbf{r}_a)\tau - \gamma_a(\mathbf{r}_a)|\tau|}, \quad (12)$$

where $\tilde{\omega}_a \equiv \tilde{\omega}_{eg}$ and $\gamma_a \equiv \gamma_{eg}$ and we have used the symmetry property $\underline{C}^\dagger(\tau) = \underline{C}(-\tau)$ (see after Eq. (6)) to extend the result to negative τ. This implies that the stationary limit of Eq. (4) is given by

$$F_{\mathrm{CP}}^{\mathrm{QRT}} = \mathrm{Re}\left[\frac{2}{\pi}\int_0^\infty d\omega\, \frac{\mathrm{Tr}\left[\mathbf{dd}\cdot\partial_z \underline{G}_I(\mathbf{r}_a,\mathbf{r},\omega)_{|\mathbf{r}=\mathbf{r}_a}\right]}{\omega + \tilde{\omega}_a(\mathbf{r}_a) - \mathrm{i}\gamma_a(\mathbf{r}_a)}\right]. \quad (13)$$

Using the symmetry properties of the Green tensor, we can rewrite Eq. (13) as an integral along the imaginary axis (see Appendix D)

$$F_{\mathrm{CP}}^{\mathrm{QRT}} = \frac{\hbar}{\pi}\int_0^\infty d\xi\, \mathrm{Tr}\Bigg[\left(\frac{\underline{\alpha}^{(2)}(\mathrm{i}\xi,\mathbf{r}_a) + \underline{\alpha}^{(2)}(-\mathrm{i}\xi,\mathbf{r}_a)}{2}\right) \cdot \partial_z \underline{G}(\mathbf{r}_a,\mathbf{r},\mathrm{i}\xi)_{|\mathbf{r}=\mathbf{r}_a}\Bigg], \quad (14)$$

where

$$\underline{\alpha}^{(2)}(\omega,\mathbf{r}_a) = \frac{\mathbf{dd}}{\hbar}\frac{2\tilde{\omega}_a(\mathbf{r}_a)}{\tilde{\omega}_a^2(\mathbf{r}_a) - (\omega + \mathrm{i}\gamma_a(\mathbf{r}_a))^2} \quad (15)$$

denotes the standard atomic polarizability tensor for a two-level atom computed in fourth-order perturbation theory [12, 38–40]. To some extent, $\underline{\alpha}^{(2)}(\omega,\mathbf{r}_a)$ can be regarded as a generalization to higher orders of perturbation theory of the corresponding (second order in $\mathbf{d}$) bare polarizability $\underline{\alpha}^{(0)}(\omega) = (2\omega_a/\hbar)\mathbf{dd}\left[\omega_a^2 - (\omega + \mathrm{i}0^+)^2\right]^{-1}$ (the small imaginary part in the denominator is introduced in order to enforce causality). Equation (14) was first derived in [12] using the QRT approach.

Upon comparing the expression for the Casimir-Polder force obtained with the QRT, Eq. (14), with that obtained using the FDT, Eq. (10), we note that they only coincide at the lowest order in perturbation theory, or, equivalently, when the polarizabilities in both equations are replaced by the bare polarizability. At higher orders they clearly differ because of the drastically distinct methods used to calculate the stationary two-point dipole correlation tensor $\underline{C}(\tau)$. The first and most evident difference is in the dependence of F_{CP} on the spectral linewidth of the polarizability: Compared to the result in Eq. (10), with $\underline{\alpha}(\omega,\mathbf{r}_a) \approx \underline{\alpha}^{(2)}(\omega,\mathbf{r}_a)$, the force resulting from Eq. (14) is less sensitive to the radiative decay

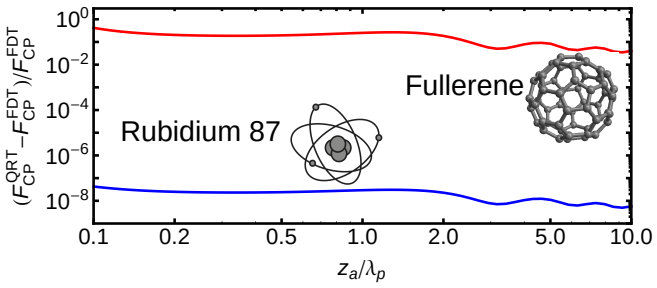

FIG. 2: Non-Markovian correction to the Casimir-Polder force as a function of the atom-surface separation, estimated as the difference between the QRT and the FDT approach (see main text). The two curves correspond to different values of the atom-field coupling: The lower (blue) curve refers to ^{87}Rb, for which the ratio between the free-space line-width and frequency is $\gamma_a^{\rm free}/\omega_a = 5\times10^{-8}$ ($\omega_a \approx 2.4\times10^{15}$ rad/s) [42]; the upper (red) curve is the result for $\gamma_a^{\rm free}/\omega_a = 1/3$, typical of fullerene (for C_{60} $\omega_a \approx 8.9\times10^{15}$ rad/s, see Ref. [41]). The behavior at large separations is associated with the oscillations of the decay rates in the retarded regime $z_a c/\omega_a \gg 1$. The planar surface is modeled as a metallic half-space whose constituent material is described by the Drude model $\epsilon(\omega) = 1-\omega_p^2[\omega(\omega+{\rm i}\Gamma)]^{-1}$ with parameters that are typical for gold: $\omega_p = 9$ eV and $\Gamma/\omega_p = 5\times10^{-3}$. The distance is measured in units of the plasma wavelength $\lambda_p = 2\pi c/\omega_p$ (~ 140 nm).

rate and its magnitude only slightly deviates from the result obtained using the bare polarizability. The application of the QRT results in a force whose magnitude is larger than that obtained via the FDT, and the difference is more pronounced for atoms with larger dipole moment (stronger atom-field coupling) [41]. We depict this behavior in Fig 2, where we compare the FDT- and QRT-based predictions using the polarizability in Eq. (15) (for simplicity we neglected the surface-induced frequency shift). We want to stress that while the approach using the QRT requires the Born-Markov approximation, only the Markov approximation is responsible for the exponential behavior of the correlation function. In the next section we show how this point is relevant to understand the difference with respect to the FDT approach.

C. Relation between the FDT and the QRT

The results of the previous two sub-sections demonstrate that the use of two of the most popular approaches for calculating quantum correlators lead to different results for the Casimir-Polder force beyond leading order. It is important to emphasize that while the FDT is an exact theorem, the QRT is based on approximations. It has already been pointed out that, because of the Born-Markov approximation, the QRT may lead to results that are incompatible with the statistical mechanics of quantum systems when treated beyond the weak-coupling approximation or perturbed far away from resonance [31, 32]. The quantum-regression theorem has proven to be remarkably successful for driven quantum optical systems, where its range of validity, near resonance, is not an impediment [33–35]. However, because of the broadband nature of electromagnetic fluctuation-induced interactions, this limited range of validity makes the QRT in general inadequate to treat such interactions. An inappropriate description of any part of the spectrum can lead to erroneous results.

Notice that, recently, in an attempt to quantify the dynamical properties of an open quantum system [6, 7], the failure of the QRT has also been proposed and investigated as a measure of the system's degree of non-Markovianity [43–45]. As seen above, the exponential behavior in the correlator obtained by applying the QRT is a direct consequence of the Markov approximation. It is well known, however, that this behavior is incorrect at large times, where the exponential decay of the correlations transforms to power-law decay [46, 47]. This difference has already been investigated in other contexts of quantum optics, e.g., the dynamics of the quantum harmonic oscillator [32] or the spontaneous decay of an excited atom in the electromagnetic vacuum [46, 48–50]. This phenomenon is related to the limitations of the Wigner-Weisskopf approximation [51, 52], which, in turn, is equivalent to the Markov approximation [46, 47]. On the other hand, it is also known that for short times the decay process starts quadratically in τ instead of the linear behavior associated with an exponential law [53]. Consequently, when one goes from the time to the frequency domain, the Fourier transform of the correlator obtained using the QRT becomes imprecise both at low and high frequencies [32].

To further understand how non-Markovian effects (manifesting as a deviation from the large-time exponential decay of the correlator) are responsible for the difference between the two expressions for the Casimir-Polder force, it is convenient to examine with some detail the two-time correlator $\underline{C}(\tau)$ in the limit of large times. According to Eq. (4) and the FDT, the relevant (symmetric) part of this quantity for $F_{\rm CP}$ is given by ($\tau > 0$)

$$\begin{aligned}\underline{C}^{\rm s}(\tau) &= \frac{\hbar}{\pi}\int_0^\infty d\omega e^{-{\rm i}\omega\tau}\underline{\alpha}_I^{\rm s}(\omega)\\ &= -\hbar\sum_\mu {\rm Res}[\underline{\alpha}^{\rm s}(\Omega_\mu)]e^{-{\rm i}\Omega_\mu\tau}\\ &\quad -{\rm i}\frac{\hbar}{\pi}\int_0^\infty d\xi e^{-\xi\tau}[\underline{\alpha}_I^{\rm s}(\omega)]_{|\omega=-{\rm i}\xi+0^+}\ , \end{aligned} \quad (16)$$

where, for simplicity, we have suppressed the dependence of the polarizability on $\mathbf{r}_a$. The second line is obtained by computing the ω integral using a contour in the lower right quadrant of the complex frequency plane. Here, "Res" denotes the residue, and $\Omega_\mu = \Omega_\mu(\mathbf{r}_a)$ are the complex poles of the polarizability. As these poles are located in the lower right quadrant, we can write $\Omega_\mu = \omega_\mu(\mathbf{r}_a) - {\rm i}\gamma_\mu(\mathbf{r}_a)$, where $\omega_\mu(\mathbf{r}_a)$ and $\gamma_\mu(\mathbf{r}_a)$ are two real and positive functions which are related to the eigen-

values of the matrix $\mathcal{M}_{ij}^{nm}$ defined at the beginning of Sec. II B. At this point, we would like to note that, for simplicity, we have assumed that the polarizability has no other discontinuity but isolated poles in the complex plane. If this were not the case, e.g., when branch cuts would be present, they must be added to Eq.(16). For the present case of simple poles, we see that the stationary dipole correlation, as given by the FDT, contains a decaying exponential behavior just like the QRT (first term in Eq.(16)), *plus* an extra term which is ultimately responsible for the difference between Eqs. (10) and (14). Upon an analytical continuation, one has

$$[\underline{\alpha}_I^{\rm s}(\omega)]_{|\omega=-{\rm i}\xi+0^+} = -\frac{\underline{\alpha}^{\rm s}({\rm i}\xi)-\underline{\alpha}^{\rm s}(-{\rm i}\xi)}{2{\rm i}}. \qquad (17)$$

This expression yields the terms that are missing in Eq.(14) in order to recover Eq.(10) (see Appendix D). While the exponential terms $\exp[-{\rm i}\Omega_\mu\tau]$ in Eq.(16) are sensitive to the details of the polarizability for frequencies around the poles Ω_μ, the last integral in Eq. (16), when $\tau\to\infty$, is sensitive to the behavior of the polarizability at low frequencies, $|\omega|\sim 0$. From the crossing relation, we know that $\underline{\alpha}_I^{\rm s}(\omega)$ is odd in frequency, which means that its form is $\underline{\alpha}_I^{\rm s}(\omega)\approx a_{2m+1}\omega^{2m+1}$ $(m=0,1,2,\dots)$. As a result, for times τ for which the exponentially decaying terms have died out, i.e., when $\tau\gg 1/\min(\gamma_i)$, the stationary correlation behaves as

$$\underline{C}^{\rm s}(\tau)\approx\frac{\hbar}{\pi}a_{2m+1}(-1)^{m+1}\frac{(2m+1)!}{\tau^{2(m+1)}}. \qquad (18)$$

The above discussion shows that for large τ the equilibrium correlation function predicted by the FDT exhibits a power-law decay instead of an exponential behavior (as would result from the QRT (see Eq.(12)).

Alternatively one can also look at the behavior of $\underline{S}(\omega)$. The power spectrum obtained from the QRT dipole correlation in Eq. (12),

$$\underline{S}_{\rm QRT}(\omega)=\frac{\mathbf{dd}}{\pi\tilde{\omega}_a}\frac{\gamma_a\tilde{\omega}_a}{(\tilde{\omega}_a-\omega)^2+\gamma_a^2}, \qquad (19)$$

does not satisfy the FDT at low frequencies: It does not vanish for $\omega\leq 0$ unlike the FDT power spectrum (Eqs. (8) and (15)). In Fig. 3 we compare $\underline{S}_{\rm QRT}(\omega)$ with the corresponding FDT power spectrum. We see that the largest difference occurs in the region $\omega\sim 0$, while around the resonance value the two expressions overlap. Notice that the impact of this inaccurate description and the resulting discrepancies only appear for evaluations at orders higher than the second, i.e. when radiative damping induced by the interaction with electromagnetic field is nonzero (see inset of Fig. 3).

In the next section, we will discuss the quantum frictional force experienced by an atom flying parallel to the surface. We will see how the above discussion about the FDT vs the QRT will play an even more relevant role in determining the correct expression for this force.

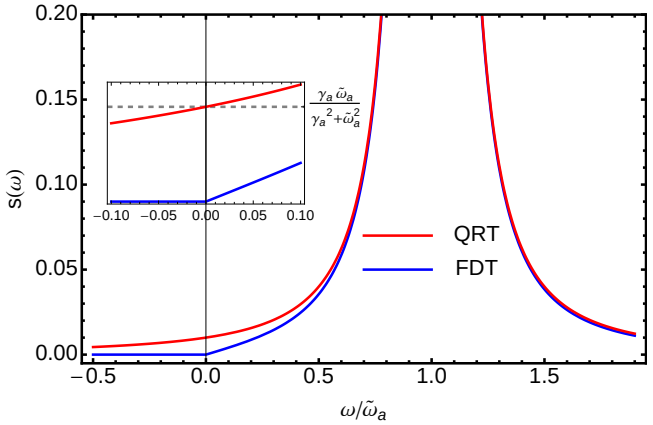

FIG. 3: Comparison of the normalized power spectra $s(\omega)=\underline{S}\cdot(\mathbf{dd}/\pi\tilde{\omega}_a)^{-1}$ predicted by the FDT (blue line) and the QRT (red line) for the polarizability of Eq. (15) (dissipation is set to $\gamma_a/\tilde{\omega}_a=10^{-2}$). While the two results are indistinguishable on resonance, they differ at low and negative frequencies. This is clearly visible in the inset, which provides a close up around $\omega=0$. While the power spectrum given by the FDT vanishes for $\omega\leq 0$, that obtained from the QRT is nonzero.

III. NON-MARKOVIAN EFFECTS IN QUANTUM FRICTION

In the previous section we have shown how non-Markovianity impacts the static atom-surface dispersive interaction. In this section we generalize our analysis to an atom moving with constant velocity $\mathbf{v}$ parallel to a planar surface. The atom then experiences a frictional force parallel to the surface that slows down its motion. Our goal is to evaluate the impact of non-Markovian effects on this force. For simplicity we will consider the case $T=0$, i.e., quantum friction.

A. Derivation of the quantum frictional force

Let us considere a prescribed trajectory $\mathbf{r}_a(t)$ for the atom. For simplicity, we focus again on an internal dynamics involving only the electric dipole moment and we neglect the magnetic moment which is a good approximation in the near field (non-retarded) region when the atom-surface distance is smaller than the relevant transition wavelengths [54]. Assuming that the surface lies in the plane $z=0$ and that the motion takes place at a constant distance z_a from the surface (see Fig. 4), the equation of motion for the atom's center of mass is $m\ddot{\mathbf{r}}_a(t)=\mathbf{F}_{\rm ext}+\mathbf{F}_{\rm fric}(t)$, where $\mathbf{F}_{\rm ext}$ is a constant external classical force and

$$\mathbf{F}_{\rm fric}(t)=\sum_i\langle\hat{d}_i(t)\nabla_\parallel\hat{E}_i(\mathbf{r}_a(t),t)\rangle. \qquad (20)$$

Here, $\nabla_\parallel\equiv(\partial_x,\partial_y)$ is the gradient parallel to the surface. Eventually, when $\mathbf{F}_{\rm ext}+\mathbf{F}_{\rm fric}(t)=0$, the system reaches a non-equilibrium steady state (NESS) given by $\mathbf{r}_a(t)=(\mathbf{R}_a+\mathbf{v}t,z_a)$ (for a discussion of the influence of the

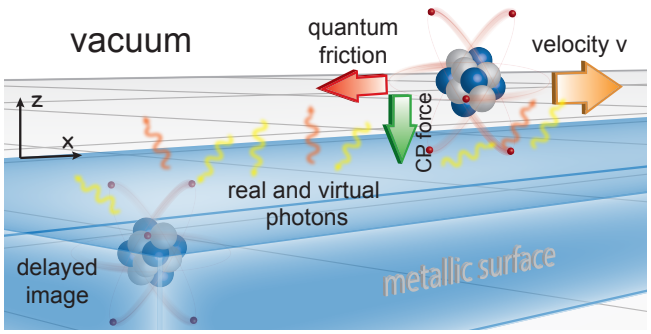

FIG. 4: Schematic of quantum friction on an atom moving at constant velocity parallel to a surface. As in the static case, the presence of the correlation tensor in the expression of the frictional force can be qualitatively understood as stemming from the interaction of the atom with its delayed image within the material.

boost on a perturbative calculation of quantum friction, we refer to [55, 56]).

Once again, similar to Eq. (2), the total field exhibits a component $\hat{\mathbf{E}}_0$ that is only related to the dissipative medium. In the dynamical case, however, due to the Doppler shift, this field mixes positive and negative frequency components when evaluated along the atom's trajectory. A splitting into annihilation and creation operators, defined in the rest frame of the surface, is still possible and we therefore write $\hat{\mathbf{E}}_0(\mathbf{r}(t),t) = \hat{\mathbf{E}}_0^{\oplus}(\mathbf{r}(t),t) + \text{h.c.}$ [55, 57], where

$$\hat{\mathbf{E}}_0^{\oplus}(\mathbf{r}(t),t) = \int_0^\infty \frac{d\omega}{2\pi} \int \frac{d^2\mathbf{k}}{(2\pi)^2} \hat{\mathbf{E}}_0(\mathbf{k}, z_a; \omega) e^{\mathrm{i}[\mathbf{k}\cdot\mathbf{R}_a(t) - \omega t]} \,. \tag{21}$$

For $\omega > 0$, the function $\hat{\mathbf{E}}_0(\mathbf{k}, z_a; \omega)$ contains the same annihilation operators as in the static case. Applying the same arguments as in the previous section, the contribution of $\hat{\mathbf{E}}_0^{\oplus}$ vanishes identically [55, 57], and we arrive at the following expression for the frictional force (see also Eq. (3)):

$$\mathbf{F}_{\text{fric}}(t) = \text{Re}\Bigg(\frac{2\mathrm{i}}{\pi} \int_0^\infty d\omega \int_0^{t-t_i} d\tau e^{-\mathrm{i}\omega\tau} \int \frac{d^2\mathbf{k}}{(2\pi)^2} \mathrm{i}\mathbf{k} \times \text{Tr}\left[\underline{C}(t, t-\tau) \cdot \underline{G}_{\Im}^{\mathsf{T}}(\mathbf{k}, z_a, \omega) \right] e^{\mathrm{i}\mathbf{k}\cdot[\mathbf{R}_a(t) - \mathbf{R}_a(t-\tau)]} \Bigg) \,. \tag{22}$$

Here, we have defined $\underline{G}_{\Im}(\mathbf{k}, z, \omega) = [\underline{G}(\mathbf{k}, z, \omega) - \underline{G}^{\dagger}(\mathbf{k}, z, \omega)]/(2\mathrm{i}) = \underline{G}_I^{\text{s}}(\mathbf{k}, z, \omega) - \mathrm{i}\underline{G}_R^{\text{as}}(\mathbf{k}, z, \omega)$. From the properties of the Green tensor (see Appendix A), we can also deduce that the symmetric part of the Green tensor is even in $\mathbf{k}$, while the antisymmetric part is odd in $\mathbf{k}$.

Owing to the dissipative properties of the system, we expect that it has a finite memory time τ_c, so that the largest contributions in the τ-integral in Eq. (22) stem from times $\tau = t - t' \lesssim \tau_c$. In particular, this means that in the limit of large times $t \to \infty$ which we will consider below, we are allowed to replace $\mathbf{R}(t)$ by $\mathbf{R}_a + \mathbf{v}t$, and $\mathbf{R}(t-\tau)$ can be approximated by $\mathbf{R}_a + \mathbf{v}(t-\tau)$. One of the main differences with respect to the static case is that now the stationary correlation tensor depends on the final velocity $\mathbf{v}$ through the state of the atom: $\underline{C}(\tau) = \lim_{t\to\infty} \langle \hat{\mathbf{d}}(t)\hat{\mathbf{d}}(t-\tau)\rangle = \text{tr}\left[\hat{d}_i(\tau)\hat{d}_j(0)\hat{\rho}_{\text{NESS}}\right] \equiv \underline{C}(\tau; \mathbf{v})$. Owing to the stationarity of the process, the correlation tensor depends once again only on the time difference τ. In the NESS, the frictional force becomes constant $\mathbf{F}_{\text{fric}}(t \to \infty) = \mathbf{F}_{\text{fric}}$, and takes the form

$$\mathbf{F}_{\text{fric}} = -\text{Re}\Bigg(\frac{2}{\pi} \int_0^\infty d\omega \int \frac{d^2\mathbf{k}}{(2\pi)^2} \mathbf{k} \int_0^\infty d\tau e^{-\mathrm{i}(\omega - \mathbf{k}\cdot\mathbf{v})\tau} \times \text{Tr}\left[\underline{C}(\tau; \mathbf{v}) \cdot \underline{G}_{\Im}^{\mathsf{T}}(\mathbf{k}, z_a, \omega) \right] \Bigg) . \tag{23}$$

In analogy with the static case, we define the power spectrum tensor

$$\underline{S}(\omega; \mathbf{v}) = \frac{1}{2\pi} \int_{-\infty}^{\infty} d\tau e^{\mathrm{i}\omega\tau} \underline{C}(\tau; \mathbf{v}). \tag{24}$$

Since $\underline{C}^{\dagger}(\tau; \mathbf{v}) = \underline{C}(-\tau; \mathbf{v})$, the power spectrum is still a Hermitean tensor $\underline{S}^{\dagger}(\omega; \mathbf{v}) = \underline{S}(\omega; \mathbf{v})$ indicating once again that its real part is a symmetric tensor and its imaginary part is an anti-symmetric tensor. Using these symmetry properties of the power spectrum, together with those of $\underline{G}_{\Im}$, we can rewrite Eq.(23) as the sum of two contributions, $\mathbf{F}_{\text{fric}} = \mathbf{F}_{\text{fric}}^{(1)} + \mathbf{F}_{\text{fric}}^{(2)}$, where

$$\mathbf{F}_{\text{fric}}^{(1)} = -2 \int_0^\infty d\omega \int \frac{d^2\mathbf{k}}{(2\pi)^2} \mathbf{k} \times \text{Tr}\left[\underline{S}_R(\mathbf{k}\cdot\mathbf{v} - \omega; \mathbf{v}) \cdot \underline{G}_I^{\text{s}}(\mathbf{k}, z_a, \omega) \right] , \tag{25}$$

and

$$\mathbf{F}_{\text{fric}}^{(2)} = 2 \int_0^\infty d\omega \int \frac{d^2\mathbf{k}}{(2\pi)^2} \mathbf{k} \times \text{Tr}\left[\underline{S}_I(\mathbf{k}\cdot\mathbf{v} - \omega; \mathbf{v}) \cdot \underline{G}_R^{\text{as}}(\mathbf{k}, z_a, \omega) \right] . \tag{26}$$

For simplicity, we model the dipole operator as $\hat{\mathbf{d}}(t) = \mathbf{d}\hat{q}(t)$. In this case $C_{ij}(\tau; \mathbf{v}) = d_i d_j \langle \hat{q}(\tau)\hat{q}(0)\rangle_{\text{NESS}}$, resulting in a symmetric power spectrum and hence $\underline{S}_I(\omega; \mathbf{v}) = 0$. This implies that for this model $\mathbf{F}_{\text{fric}}^{(2)} = 0$. The physical meaning of the term $\mathbf{F}_{\text{fric}}^{(2)}$ will be discussed in a more general context in a future work.

At this point, and within our assumptions, Eq.(25) is exact. It gives the quantum frictional force on an atom that asymptotically moves at constant velocity parallel to the surface. In order to evaluate this force, we need to compute the non-equilibrium power spectrum tensor $\underline{S}(\omega; \mathbf{v})$. Unfortunately, this calculation is a complex problem which often can be addressed only within perturbation theory. In the following, we describe two different approaches based on the FDT and the QRT, which yield markedly different predictions for the quantum friction in the low-velocity limit. This allows us to assess the impact of non-Markovianity on non-equilibrium fluctuation-induced interactions.

B. FDT in quantum friction

Strictly speaking, it is not valid to use the FDT for the problem of a moving atom above a surface since the system's steady state is not in equilibrium [58]. Nevertheless, earlier works [54, 59–61] have (implicitly or explicitly) relied on the FDT to calculate quantum friction, assuming that both the atom and the surface are *locally* in thermal equilibrium (LTE). Although the LTE approximation has been used in the literature for several non-equilibrium fluctuation-induced interactions (e.g., radiative heat transfer [62] or static atom-surface and Casimir forces out-of-thermal equilibrium [63]), its justification is still a matter of discussion. In Ref. [58] we proved for a specific system that the local thermal equilibrium approximation actually *fails* in the case of quantum friction. Interestingly, however, we are going to show below that in the general case it is still possible to draw conclusions on the low-velocity behavior of the frictional force [64].

For symmetry reasons an expansion of the friction force for low velocities must contain only odd powers of v. As $\underline{G}_I^{\rm s}(\mathbf{k}, z_a, \omega)$ is even in $\mathbf{k}$, the frictional force in Eq.(25) identically vanishes for $\mathbf{v} = 0$, as it should. Also, as the dipole power spectrum explicitly depends on the wave vector only through the Doppler-shifted frequency $\omega' = \omega - \mathbf{k}\cdot\mathbf{v}$, only two terms in Eq.(25) can contribute to the drag force in the small velocity limit. The first term is that in which we set the explicit $\mathbf{v}$-dependence to zero in the Doppler shift and retain the implicit velocity-dependence through the NESS density matrix, i.e., $\underline{S}_R(-\omega;\mathbf{v})$. The second term is that in which we set $\mathbf{v} = 0$ in the implicit velocity-dependence and retain the Doppler shift, i.e., $\underline{S}_R(-\omega';\mathbf{v}=0)$. The first term does not contribute to the low-velocity drag force because the integral over $\mathbf{k}$ in Eq.(25) identically vanishes as $\underline{G}_I^{\rm s}(\mathbf{k}, z_a, \omega)$ is even in $\mathbf{k}$. The factor $\underline{S}_R(-\omega';\mathbf{v}=0)$ in the second term is identical to the static power spectrum with negative Doppler-shifted frequency. Because it effectively corresponds to an equilibrium situation ($\mathbf{v} = 0$), its contribution to Eq.(25) can be computed using the corresponding FDT [Eq.(8)]

$$\underline{S}_R(-\omega';\mathbf{v}=0) = \frac{\hbar}{\pi}\theta(-\omega')\underline{\alpha}_I(-\omega'), \tag{27}$$

where $\underline{\alpha}$ is the polarizability tensor for the atom *at rest*. Eq. (27) is a simplification of Eq. (8) because in our dipole model the polarizability and the dipole correlator are symmetric by assumption.

Since the surface is invariant under rotations around the z-axis, in the following we assume without loss of generality that the surface-parallel motion occurs in the x-direction, i.e., $\mathbf{v} = v_x\mathbf{x}$ ($\mathbf{x}$ is the unit vector along the x-direction), which, considering again the parity properties of the Green tensor and symmetry of our system, implies that $\mathbf{F}_{\rm fric} = F_{\rm fric}\mathbf{x}$. Based on the arguments in the previous paragraph, any linear order in the velocity is included in

$$F_{\rm fric} \approx -\frac{2\hbar}{\pi}\int_{-\infty}^{\infty}\frac{dk_y}{2\pi}\int_0^{\infty}\frac{dk_x}{2\pi}k_x\int_0^{k_x v_x} d\omega \times \mathrm{Tr}\left[\underline{\alpha}_I(k_x v_x - \omega;0)\cdot\underline{G}_I(\mathbf{k}, z_a, \omega)\right] . \tag{28}$$

At this point it is important to clarify the role played by the different terms in the above expression. The cut-off in the ω-integral and the restriction to positive k_x is due to the Heaviside function $\theta(-\omega') = \theta(k_x v_x - \omega)$ in Eq. (27): this enforces a vanishing power spectrum for positive Doppler-shifted frequencies, revealing an important part of the underlying physics involved in the quantum friction process. When $v_x = 0$, $\omega' = \omega > 0$ and the Heaviside $\theta(-\omega')$ function identically vanishes, explaining why the frictional force is zero at zero velocity. However, due to the motion, we have that $\omega' = \omega - k_x v_x < 0$ in the interval $0 < \omega < k_x v_x$, which results in a nonzero contribution to the integral in Eq.(28). The so-called anomalous Doppler-effect [65, 66] occurs in this region, where part of the kinetic energy of the atom is converted into real excitations. (This mechanism is very much related to the physics of the Vavilov-Cherenkov effect [60, 67–70].) The remaining terms in Eq.(28) are connected to the interaction strength and they essentially describe the density of states for the atomic system ($\underline{\alpha}_I$) and for the electromagnetic field emitted by the surface ($\underline{G}_I$).

Because they are odd, the imaginary parts of both susceptibilities vanish at $\omega = 0$, and since the Green tensor limits the values of wave vectors to $|\mathbf{k}| \lesssim z_a^{-1}$, an expansion at the lowest order in v_x gives

$$F_{\rm fric} \approx -\frac{2\hbar v_x^3}{3(2\pi)^3}\int_{-\infty}^{\infty}dk_y\int_0^{\infty}dk_x\, k_x^4 \mathrm{Tr}\left[\underline{\alpha}_I'(0)\cdot\underline{G}_I'(\mathbf{k}, z_a, 0)\right] . \tag{29}$$

Here, assuming the existence of some inherent form of dissipation (see also Sec. IV below), we have considered that the first derivative in ω (indicated by the prime in the above expression) of both tensors does not vanish (Ohmic behavior). Note that when either $\underline{\alpha}_I'(0)$ or $\underline{G}_I'$ are zero, higher (odd) orders in v_x appear in the expansion. A more quantitative evaluation of Eq. (29) requires the atom's low-frequency polarizability or dipole spectrum (see for example Fig. 3), which is known within the limits of perturbation theory [12, 38–40] (see also Section IV).

The above arguments demonstrate that, within our description of the atom, independently of the details of the internal dynamics (e.g. linear or non-linear, induced or intrinsic dissipation), the lowest-order expansion in velocity of the zero-temperature stationary frictional force on an atom moving above a planar surface is at least cubic in v_x. This outcome is in agreement with some of the results available in the literature [2, 3], and it is formally equivalent to the application of the LTE approximation. There are, however, a few points that distinguish our approach from the use of that approximation. First, the derivation of Eq. (29) provides a framework and a plausibility argument for the application of the LTE approach to the quantum friction problem. Nonetheless

in Eq. (29), there can be other v_x^3 contributions to the frictional force arising from the intrinsic non-equilibrium velocity-dependence of the power spectrum $S(\omega;\mathbf{v})$. As shown in Ref. [58], such additional v_x^3-contributions do exist for the case of an atom modeled as a harmonic oscillator, which, as already said before, demonstrates in this case the failure of the LTE approximation in quantum friction. Second, the dependence on v_x^3 is a consequence of a general property of the polarizability, the crossing relation, and its behavior at low frequencies. This shows that, at least for the case of surface-parallel motion, the low velocity behavior of quantum friction is not qualitatively related to the details of the (velocity-modified) internal dynamics, e.g. velocity dependent damping rates or level shifts [40, 57, 71].

C. QRT in quantum friction

We now compute the friction force at low velocities predicted by the QRT formula. From the previous subsection and II C, we may expect a quite different behaviour because of the dependency of the polarizability at low frequencies.

Our starting point is Eq. (23). Following our discussion in the previous sub-section, in the low-velocity limit one can approximate the correlator $\underline{C}(\tau;\mathbf{v})$ by the static correlator $\underline{C}(\tau;\mathbf{v}=0)$, and only retain the velocity-dependence in the Doppler shift (the $\exp[-\mathrm{i}(\omega-\mathbf{k}\cdot\mathbf{v})\tau]$ factor in Eq.(23)). As a result, in order to compute the frictional force Eq. (23), we need to evaluate the quantity

$$\mathrm{Re}\int_0^\infty d\tau e^{-\mathrm{i}(\omega-\mathbf{k}\cdot\mathbf{v})\tau}\underline{C}(\tau;0) = \underbrace{\hbar\mathrm{Re}\sum_\mu\left(\frac{\mathrm{iRes}[\underline{\alpha}(\Omega_\mu)]}{\Omega_\mu+\omega-\mathbf{k}\cdot\mathbf{v}}\right)}_{\underline{S}_{\mathrm{QRT}}(\mathbf{k}\cdot\mathbf{v}-\omega)} \underbrace{-\hbar\mathrm{Re}\sum_\mu\left(\frac{\mathrm{iRes}[\underline{\alpha}(\Omega_\mu)]}{\Omega_\mu+|\omega-\mathbf{k}\cdot\mathbf{v}|}\right)}_{\underline{S}_{\mathrm{nM}}(\mathbf{k}\cdot\mathbf{v}-\omega)}. \quad (30)$$

(For simplicity we consider the case where both the correlation and the polarizability tensors are symmetric.) The static correlation tensor, computed with the FDT, is given in Eq.(16). We recall that the first term of the sum in Eq. (16) corresponds to the exponential decay and is the result one would have obtained via the QRT expression for the static correlator (such as Eq. (12) for the two-level system). After performing the relevant integral, this term gives rise to the contribution $\underline{S}_{\mathrm{QRT}}(\mathbf{k}\cdot\mathbf{v}-\omega)$ in Eq.(30). The second contribution in Eq.(30) arises from the last term of the correlator in Eq.(16), which contains the non-Markovian (nM) behavior and yields the long time deviation from the decaying exponential. With the assumption that the polarizability is a symmetric tensor, we can formally write $\underline{\alpha}(\omega) = \sum_\mu\{\mathrm{Res}[\underline{\alpha}(\Omega_\mu)]/(\omega-\Omega_\mu)-\mathrm{Res}[\underline{\alpha}(-\Omega_\mu^*)]/(\omega+\Omega_\mu^*)\}$, from which we obtain

$$\frac{\underline{\alpha}(\mathrm{i}\xi)-\underline{\alpha}(-\mathrm{i}\xi)}{2\mathrm{i}} = -\xi\sum_\mu\left\{\frac{\mathrm{Res}[\underline{\alpha}(\Omega_\mu)]}{\xi^2+\Omega_\mu^2}-\frac{\mathrm{Res}[\underline{\alpha}(\Omega_\mu)]^*}{\xi^2+\Omega_\mu^{*2}}\right\}. \quad (31)$$

Performing the relevant integrals in Eqs. (16) and (30), we obtain $\underline{S}_{\mathrm{nM}}(\mathbf{k}\cdot\mathbf{v}-\omega)$. This analysis reveals that the two terms $\underline{S}_{\mathrm{QRT}}$ and $\underline{S}_{\mathrm{nM}}$ are very similar, and cancel each other for $\omega' = -(\omega-\mathbf{k}\cdot\mathbf{v}) < 0$. We shall see now that both contributions are relevant for the final expression of the frictional force.

Let us consider the first term $\underline{S}_{\mathrm{QRT}}$ in Eq.(30) and derive the corresponding QRT form of quantum friction at low velocities. Using that $|\mathbf{k}| \lesssim z_a^{-1}$ and again assuming without loss of generality that the motion is along the x-axis, to the lowest order in v_x ($v_x \ll \min[|\Omega_\mu|]z_a$), we obtain

$$F_{\mathrm{fric}}^{\mathrm{QRT}} \approx -\frac{4\hbar v_x}{(2\pi)^2}\int_0^\infty d\omega\int_{-\infty}^\infty dk_y\int_0^\infty dk_x\, k_x^2 \times \mathrm{Tr}\left[\sum_\mu \mathrm{Re}\left[\frac{\mathrm{iRes}[\underline{\alpha}(\Omega_\mu)]}{(\Omega_\mu+\omega)^2}\right]\cdot\underline{G}_I(\mathbf{k},z_a,\omega)\right]. \quad (32)$$

This means that at low velocities the QRT predicts a frictional force linear in the velocity of the atom [55, 57]. This result contrasts with the cubic dependence in v_x in Eq. (28).

The difference between these two outcomes is due to the behavior of $\underline{S}(\omega)$ at low frequencies (see Section II C and in particular Fig. 3). Mathematically, this can be understood by considering the contribution of $\underline{S}_{\mathrm{nM}}(\mathbf{k}\cdot\mathbf{v}-\omega)$ to Eq.(23): A direct calculation of the frictional force that originates from this term, results in an expression that leads to a linear-in-v_x part which cancels the contribution in Eq.(32) (see Appendix E). Thus, a higher-order expansion is required and, by symmetry, the next order to be considered is cubic in v_x. Alternatively one can say that the main effect of $\underline{S}_{\mathrm{nM}}(\mathbf{k}\cdot\mathbf{v}-\omega)$ is to limit the range of integration over frequency to $0<\omega<\mathbf{k}\cdot\mathbf{v}$ as in Eq. (28). Since $\underline{S}_{\mathrm{QRT}}(0)+\underline{S}_{\mathrm{nM}}(0)=0$ and, again, $\underline{G}_I(\mathbf{k},z_a,0)=0$ any further possible linear-in-v_x terms will vanish and an expansion for low velocities leads to Eq.(29).

IV. QUANTUM FRICTION TO SECOND-ORDER IN PERTURBATION THEORY

For a better understanding of the behavior of the frictional force, it is instructive to evaluate the interaction within second order perturbation theory in the electric dipole moment $\mathbf{d}$ following the FDT approach (see Eq. (28)). A special role is played by dissipation in the particle's internal dynamics: the second order frictional force is different depending on whether this dissipation is *induced* or *intrinsic*. In systems with induced (i.e. radiative) dissipation (e.g. atoms) at second order, quantum

friction is instead exponentially suppressed [55, 72, 73] at low velocities and the leading contribution requires a calculation at the fourth order [56, 58, 64]. In contrast, in systems with intrinsic dissipation (e.g. nano-particles), an approach at second order in the field-dipole coupling provides the leading contribution. The difference between these two cases can be once again explained by looking at the low frequency behavior of the imaginary part of the polarizability, which in systems like atoms starts to be accurately described in an approach beyond second order perturbation theory.

A. Frictional force on atoms

Within a perturbative framework at second order in the dipole moment $\mathbf{d}$, the dipole correlator $\underline{C}(\tau;\mathbf{v})$, and therefore the non-equilibrium power spectrum entering in Eq. (25), lose their explicit dependence on the velocity. At this order, the dipole correlator is calculated starting from the free evolution of the dipole operator: The system is decoupled from the electromagnetic field and, therefore, is locally in thermal equilibrium. This means that the FDT can be employed, and the frictional force takes the form of Eq. (28), where the tensor $\underline{\alpha}$ must be replaced with the bare polarizability (see discussion after Eq. (15)). We have $\underline{\alpha}_I^{(0)}(\omega) = (\mathbf{dd}/\hbar)\pi\left[\delta(\omega_a-\omega)-\delta(\omega_a+\omega)\right]$ (in this case the expansion in Eq. (29) does not hold) and inserting it in Eq.(28) this gives

$$F_{\rm fric}^{(2)} \approx -2\int_{-\infty}^{\infty}\frac{dk_y}{2\pi}\int_{\omega_a/v_x}^{\infty}\frac{dk_x}{2\pi}\,k_x \times \mathrm{Tr}\left[\mathbf{dd}\cdot\underline{G}_I(\mathbf{k},z_a,k_xv_x-\omega_a)\right]. \quad (33)$$

This expression indicates that only wave vectors $k_x > \omega_a/v_x$ contribute to the frictional force. However, since the relevant part of Green tensor is proportional to $\exp[-2kz_a] < \exp[-2\omega_a z_a/c]$ with $k=|\mathbf{k}|$ (see Appendix A), $F_{\rm fric}^{(2)}$ exponentially vanishes in the low velocity limit. To see this more clearly, we recall that the total Green tensor can be decomposed as $\underline{G} = \underline{G}_0 + \underline{g}$. Because of Lorentz invariance, the free-space contribution $\underline{G}_0$ does not contribute to the frictional force [73, 74]. The scattered part of the Green tensor $\underline{g}$ has a symmetric part (the only relevant part in Eq.(33)) whose imaginary part in the near-field regime ($z_a \ll c/\omega$) can be written as (see Appendix A)

$$\underline{g}_I(\mathbf{k},z_a;\omega) = \frac{r_I(\omega)}{2\epsilon_0}ke^{-2kz_a}\left(\frac{k_x^2}{k^2}\mathbf{xx}+\frac{k_y^2}{k^2}\mathbf{yy}+\mathbf{zz}\right), \quad (34)$$

where ϵ_0 is the vacuum permittivity. Further, $r(\omega) = [\epsilon(\omega)-1]/[\epsilon(\omega)+1]$ is the quasi-static approximation of the transverse magnetic (TM) reflection coefficient for the planar surface – here, we recall that in the near-field regime only the TM polarization matters for dielectric or metallic surfaces, and we have neglect $\mathbf{k}$ dependence of the reflection coefficient. Also, for simplicity, throughout this manuscript we neglect spatial dispersion.

Let us examine the case of a metallic surface described by the Drude model $\epsilon(\omega) = 1-\omega_p^2[\omega(\omega+\mathrm{i}\Gamma)]^{-1}$, where ω_p is the plasma frequency and Γ the metal's relaxation (dissipation) rate. In the limit of very small dissipation ($\Gamma \to 0$) we have $r_I(\omega) \approx (\pi\omega_{\rm sp}/2)\left[\delta(\omega-\omega_{\rm sp})-\delta(\omega+\omega_{\rm sp})\right]$, where $\omega_{\rm sp} = \omega_p/\sqrt{2}$ is the surface plasmon resonance. The integrals in Eq.(33) can be evaluated exactly, and the resulting second-order frictional force is

$$\frac{F_{\rm fric}^{(2)}}{F_0} = \frac{\omega_a/\omega_{\rm sp}}{12\,(v_x/c)^4}\left(1+\frac{\omega_a}{\omega_{\rm sp}}\right)^3\mathcal{K}(u,\varphi,\theta)\,, \quad (35)$$

where

$$\mathcal{K}(u,\varphi,\theta) = A_0(\varphi,\theta)K_0(2\,|u|)+A_2(\varphi,\theta)K_2(2\,|u|). \quad (36)$$

In these expressions, $u = z_a(\omega_{\rm sp}+\omega_a)/v_x$, θ and φ are respectively the polar and azimuthal spherical angles describing the dipole vector $\mathbf{d}$. In addition, $A_0(\varphi,\theta) = (3/2)\left[1+\left(3\cos^2(\varphi)-2\right)\sin^2(\theta)\right]$, $A_2(\varphi,\theta) = (3/2)\left[1-\cos^2(\varphi)\sin^2(\theta)\right]$, and $K_n(x)$ is the nth order modified Bessel function of the second kind. Equation (35) demonstrates that the frictional force depends on the orientation of the dipole vector of the atom. The largest value of $F_{\rm fric}^{(2)}$ is found for dipoles oriented normal to the surface ($\theta=0$) or, if tilted with respect to the normal, when the vector of the dipole moment exhibits a large component along the direction of the motion $\phi=0$. The minimum value occurs for dipoles oriented along the y-axis, i.e., when the vector of the dipole moment is perpendicular to both the surface normal and the atom's propagation direction (see inset of Fig.5). For simplicity, in the following we will consider expressions averaged over all dipole orientations, hence, $\bar{A}_0 = \bar{A}_2 = 1$. The normalization is $F_0 = -3\hbar\omega_{\rm sp}^5\alpha_0/(2\pi\epsilon_0c^4)$, where $\alpha_0 = 2|\mathbf{d}|^2/(3\hbar\omega_a)$ is the static atomic polarizability. As an example, using a plasma frequency $\omega_p = 9$ eV and a ^{87}Rb atom ($m = 1.44\times10^{-25}$ kg, $\alpha_0 = 5.26\times10^{-39}\mathrm{Fm}^2$ [42]), we have $F_0 \sim 0.31$ fN, corresponding to an acceleration $F_0/m \sim 2.17\times10^9$ m/s^2.

Since $K_n(x\gg1) \approx e^{-x}\sqrt{\pi/2x}$, the frictional force Eq. (35) is exponentially small at low velocities $v_x \ll z_a\omega_a$, namely

$$\frac{\bar{F}_{\rm fric}^{(2)}}{F_0} \approx \sqrt{\frac{\pi\left(\frac{\omega_a}{12\omega_{\rm sp}}\right)^2\left(1+\frac{\omega_a}{\omega_{\rm sp}}\right)^5}{\frac{\omega_{\rm sp}z_a}{c}\left(\frac{v_x}{c}\right)^7}}e^{-\left(1+\frac{\omega_a}{\omega_{\rm sp}}\right)\frac{2z_a\omega_{\rm sp}}{v_x}}. \quad (37)$$

In Fig. 5 we display the velocity dependence of the second-order quantum frictional force for a substrate with vanishingly small dissipation, Eq.(35). It grows to sensible values only for velocities $v_x > z_a\omega_a$, which follows from the constraint on the wave vector discussed above. A maximum occurs for $v_x \approx (4/7)(\omega_a+\omega_{\rm sp})z_a$, i.e., roughly when the Doppler-shifted surface-plasmon

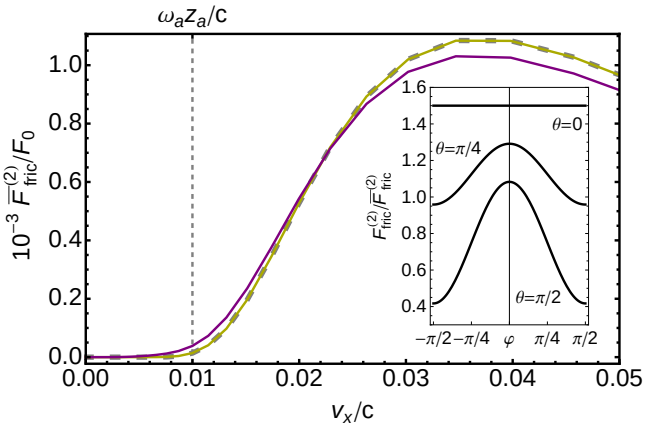

FIG. 5: Velocity dependence of the averaged second-order frictional force for a particle without intrinsic dissipation (e.g. an atom) moving above a metallic surface. The normalization is $F_0 = -3\hbar\omega_{\rm sp}^5\alpha_0/(2\pi\epsilon_0 c^4)$. The metal is described by the Drude model and results for various dissipation parameters are depicted: $\Gamma = 0$ (gray dashed, Eq. (35)), $\Gamma/\omega_{\rm sp} = 10^{-3}$ (dark yellow), and $\Gamma/\omega_{\rm sp} = 10^{-1}$ (purple). The other parameters are $\omega_a/\omega_{\rm sp} = 0.2$ and $z_a\omega_{\rm sp}/c = 0.05$, corresponding to the near-field regime, and $v_x/c = 0.04$. The inset depicts the dependence of quantum friction for $\Gamma = 0$, Eq. (35), on the orientation of the vector of the dipole moment: The value $\theta = 0$ corresponds to a dipole oriented normal to the surface; if tilted, the force has is largest value is found for a dipole in the xz-plane ($\phi = 0$).

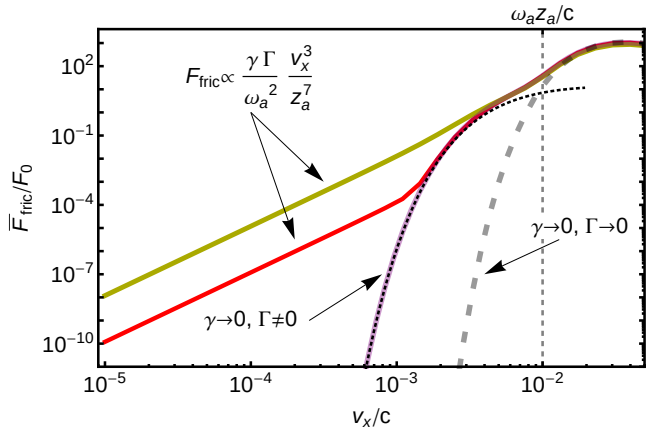

FIG. 6: Velocity dependence of the normalized averaged second-order quantum frictional force for a particle with intrinsic dissipation. The normalization is $F_0 = -3\hbar\omega_{\rm sp}^5\alpha_0/(2\pi\epsilon_0 c^4)$. The particle has an internal resonance frequency $\omega_a/\omega_{\rm sp} = 0.2$ and moves at a distance $z_a\omega_{\rm sp}/c = 0.05$ above the surface, corresponding to the near-field regime. Results for two different values of the intrinsic dissipation are displayed: $\gamma/\omega_{\rm sp} = 10^{-1}$ (dark yellow) and $\gamma/\omega_{\rm sp} = 10^{-3}$ (red). In both cases, the damping Γ is set to $\Gamma/\omega_{\rm sp} = 10^{-1}$. The purple curve shows the case for $\gamma = 0$ and $\Gamma/\omega_{\rm sp} = 10^{-1}$. The black dotted curve represents the expression in Eq.(38). The thick gray dashed curve is Eq.(35).

resonance frequency is brought into resonance with the atomic transition (the imaginary part of reflection coefficient $r(v_x/z_a - \omega_a)$ becomes large) [75]. This means that, at second order, quantum friction is essentially the result of a resonant process: The velocity must be sufficiently large (within the non-relativistic approach used here) so that the Doppler effect becomes anomalous, and the corresponding shifted frequencies are sufficiently large in order to include the (sharp) atomic transition and excite a plasmon. A photon (plasmon) in the near field is then created and the atom is temporarily excited. The peak's width in Fig. 5 is related to the broad distribution of k-vectors in Eq. (34).

When dissipation in the substrate is taken into account ($\Gamma \neq 0$), the second-order quantum frictional force still exhibits resonant behavior at high velocities ($v_x > z_a\omega_a$), as discussed above (see Fig. 5). At low frequencies, however, the imaginary part of the reflection coefficient behaves in this case as $r_I(\omega) \approx \omega\Gamma/\omega_{\rm sp}^2$. The frictional force at low velocities still decays exponentially, but acquires a different asymptotic behavior due to the modification of the electromagnetic density of states induced by dissipation in the metal. It is described by

$$\frac{\bar{F}^{(2)}_{\rm fric}}{F_0} \approx \frac{\Gamma}{24\omega_{\rm sp}}\sqrt{\frac{\left(\frac{\omega_a}{\omega_{\rm sp}}\right)^7}{\pi\left(\frac{\omega_{\rm sp}z_a}{c}\right)^5\left(\frac{v_x}{c}\right)^3}}\left(1+\frac{5v_x}{2z_a\omega_a}\right)e^{-\frac{2z_a\omega_a}{v_x}}, \tag{38}$$

which is clearly visible in Fig. 6 (black dotted curve).

B. Frictional force on nano-particles

Within the second-order perturbative approach, we can study the effect of dissipation associated with the particle's internal dynamics by considering the case of a system with intrinsic damping. Interestingly, at this order, the force on a moving object having intrinsic dissipation (e.g., a metallic nanoparticle) is qualitatively different from that on the moving atom. For this kind of system, we take as bare polarizability $\underline{\alpha}^{(0)}(\omega) = (2\mathbf{dd}/\hbar\omega_a)\omega_a^2/(\omega_a^2 - \omega^2 - {\rm i}\gamma\omega)$. For the case of a metallic nanoparticle, $\omega_a = \omega_p^{\rm np}/\sqrt{3}$ is the resonance frequency of the localized surface plasmon, and $\omega_p^{\rm np}$ and γ are, respectively, the plasma frequency and the dissipation rate for the bulk metal that comprises the particle. For this setup both the polarizability and the Green tensor have a non vanishing first derivative with respect to ω. As demonstrated in Fig. 6, when both sub-systems have finite dissipation ($\gamma \neq 0$, $\Gamma \neq 0$), at low velocity a further asymptotic appears in the force given in Eq. (29), and the frictional force is described by

$$\frac{\bar{F}^{(2)}_{\rm fric}}{F_0} \approx \frac{45}{16}\frac{\Gamma}{24\pi}\frac{\gamma}{\omega_a^2}\left(\frac{c}{\omega_{\rm sp}z_a}\right)^7\left(\frac{v_x}{c}\right)^3. \tag{39}$$

Contrary to the previous cases, the second-order quantum frictional force for systems with intrinsic dissipation

does not exponentially vanish at low velocities, but rather exhibits a cubic velocity dependence, just as predicted by Eq.(29) on the basis of general arguments [76]. In Fig. 6 we display all the three cases discussed above. Note that even when both sources of dissipation are non-zero, the quantum frictional force approaches the results of the other cases for larger velocities. Specifically, the case $\Gamma \neq 0$, $\gamma \to 0$ is approached first and this is followed by approaching the case Γ, $\gamma \to 0$. The three asymptotic expressions for low v_x derived above cannot be obtained from each other by taking $\gamma \to 0$ or $\Gamma \to 0$, indicating that these limits do not commute and that, at low velocities, dissipation is very relevant for quantum frictional processes. This behavior is directly related to the corresponding increase in the density of states at low frequencies that is induced by dissipation (cf. the discussion following Eq. (28)). Notice that, although we have calculated the last two asymptotic expressions for a Drude metal, they can easily be generalized to other media having an Ohmic behavior at low frequencies, i.e., $r_I(\omega) = 2\epsilon_0\rho\omega$ for $\omega \to 0$ where ρ is the DC resistivity (for metals described by the Drude model $\rho = \Gamma/(\epsilon_0\omega_{\rm sp})$).

Finally, let us compare Eq. (39) with the expression for the frictional force one obtains for this same configuration using the QRT. In the near-field (see Eq. (34)) and in the limits $\gamma/\omega_a \ll 1$ and $\Gamma/\omega_{\rm sp} \ll 1$, Eq. (32) gives [55, 57]

$$\frac{\bar{F}_{\rm fric}^{\rm QRT}}{F_0} \approx 2\pi \frac{\gamma\omega_a\omega_{\rm sp}}{(\omega_a+\omega_{\rm sp})^3}\left(\frac{c}{2\omega_{\rm sp}z_a}\right)^5 \frac{v_x}{c}\,. \qquad (40)$$

Besides the linear velocity-dependence behavior already discussed above, we note a distance dependence with a power law different from that in Eq. (39). Using a simple dimensional analysis one can show that this feature is connected with the low-frequency behavior of the polarizability. Equation (40) also shows that, to leading order, the force does not depend on the material dissipation. Within the QRT the frictional force is indeed dominated by a resonant process occurring at the surface plasmon frequency. In the FDT approach, leading at low velocities to Eq. (39), this resonant process can only occur for large velocities, $v_x \sim \omega_{\rm sp} z_a$, due to the limitations set by the anomalous Doppler effect (see Sec. III B and Figs. 5 and 6).

V. SUMMARY AND DISCUSSION

Using general concepts of quantum statistical mechanics, we have investigated the impact of the Markov approximation on fluctuation-induced atom-surface interactions. In the static case, we have analyzed the failure of this approximation by comparing the outcomes obtained using the FDT and the QRT. The FDT has led to a non-perturbative expression for the zero-temperature Casimir-Polder force, Eq.(10). The FDT-based result contains the previously known expressions as special cases (see Appendix B for details). We have shown that an alternative approach based on the QRT agrees with the FDT within lowest-order in perturbation theory in the atom-field coupling strength, but differs at higher orders. This can be intuitively understood by recalling that the QRT relies on the Born-Markov approximation, which works well for weak atom-field couplings and in a narrow range of frequencies close to resonance. This effectively limits the applicability of the QRT for fluctuation-induced interactions, given the broadband nature of the latter.

The difference between the FDT and the QRT becomes even more pronounced in quantum friction. Specifically, the distinct behavior at large times/low frequencies of the dipole-dipole correlation function is responsible for the different scaling laws of quantum friction with regard to atom velocity and atom-surface separation. We have shown that, when (intrinsic) Ohmic dissipation is incorporated in both, the constituent material and the atom dynamics, quantum friction scales as $\propto v_x^3$ for low velocities. By contrast, a Markovian approach leads to a behavior $\propto v_x$. More generally, the exponent of the power law at low velocities is strongly related to the low frequency behavior of the atomic and the material susceptibilities. This explains why dissipation is so relevant: quantum friction is dominated by low frequencies and there damping increases the density of states, thus opening new interaction channels.

For systems that exhibit intrinsic dissipation (e.g. a nano-particle above a surface) a second-order perturbative calculation is sufficient to compute the leading term of low-velocity quantum friction (see Sec. IV). However, for systems exhibiting only radiative damping (e.g., atoms), a consistent higher-order (fourth at least) calculation is required in order to accurately describe the quantum frictional process [55, 56, 58] .

The approach presented in this manuscript is based on stationary systems and is thus not suitable for the analysis of non-steady-state configurations, e.g., an excited atom. However, in the case of atoms it has recently been shown that in the case of non-stationary quantum friction the salient features of our results can also be recovered within a time-dependent perturbative approach to the fourth order in the atom-field coupling strength [56]. Intuitively, one can understand this result in terms of the characteristic time $\tau_{\rm NESS}$ which the system needs to reach the non-equilibrium steady state – as even within a time-dependent perturbative scheme, steady-state features become relevant as soon as we consider $t \gg \tau_{\rm NESS}$.

We conclude with some comments concerning the experimental investigation of the effects discussed above. The corrections to the Casimir-Polder force depend on the linewidth of the system's resonance (see Eq. (14)). Microscopic systems with large internal dissipation appear to be suitable candidates to detect the difference between the two approaches. Examples of such systems include metallic nano-particles [83, 84] or even large molecules like fullerene for which a difference of about 10% between the QRT and the FDT approaches is pre-

dicted (see Fig. 2). Such accuracy might require a spectroscopic analysis (see for example [85]). Since in atoms and molecules the decay rate usually increases with large polarizabilities and small atom-surface separations, experiments should aim at short-distance measurements with microscopic objects with a large electric dipole moment, such as Rydberg atoms.

In the case of quantum friction an experimental detection is more difficult due to the small value of the drag force. For example, for a metallic nanoparticle with radius $R = 2$ nm ($\alpha_0 = 4\pi\epsilon_0 R^3$), $\omega_a = 4$ eV and $\gamma = 70$ meV, moving at $v_x = 340$ m/s, at a distance $z_a = 10$ nm away from a silicon surface ($\rho = 6.4 \times 10^2\ \Omega$ m) we have that within the FDT approach $\bar{F}^{(2)}_{\rm fric} = 2.43 \times 10^{-23}$ N. As a comparison, for the same configuration, choosing $\omega_{\rm sp} \sim 7$ eV for silicon, the QRT force in Eq. (40) leads to a value which is 5×10^3 larger. A alternative approach for measuring the frictional force might rely on atom interferometry [86]: When two arms of the interferometer are placed at different distances from a surface, the friction on atoms moving along them would lead to a different phase accumulation which, in turn, would be detectable as an interference pattern [87].

VI. ACKNOWLEDGMENTS

We thank Gabriel Barton, Stefan Buhmann, Manuel Donaire, Belen Farias, Juliane Klatt, Kimball Milton, Daniel Reiche, Stefan Scheel, and Wang-Kong Tse for useful discussions. We acknowledge support by the LANL LDRD program, and by the Deutsche Forschungsgemeinschaft (DFG) through project B10 within the Collaborative Research Center (CRC) 951 Hybrid Inorganic/Organic Systems for Opto-Electronics (HIOS). FI further acknowledges financial support from the European Union Marie Curie People program through the Career Integration Grant No. PCIG14- GA-2013-631571. CH and FI acknowledge support from the DFG through the DIP program (grant FO 703/2-1)

Appendix A: Properties of the Green tensor

The electromagnetic Green tensor is the solution of

$$\left[\nabla\times\nabla\times - \frac{\omega^2}{c^2}\epsilon(\mathbf{r},\omega)\right]\underline{G}(\mathbf{r},\mathbf{r}',\omega) = \frac{\omega^2}{\epsilon_0 c^2}\delta(\mathbf{r}-\mathbf{r}'), \quad \text{(A1)}$$

subjected to appropriate boundary conditions. Some useful properties of the Green tensor are $\underline{G}^{\mathsf{T}}(\mathbf{r}_1,\mathbf{r}_2,\omega) = \underline{G}(\mathbf{r}_2,\mathbf{r}_1,\omega)$ (the superscript T indicates the transposed matrix) and $\underline{G}(\mathbf{r},\mathbf{r}',\omega) = \underline{G}^*(\mathbf{r},\mathbf{r}',-\omega)$ which are, respectively, consequences of reciprocity and the fact that in the time domain its elements are real. Further, the Green tensor represents a susceptibility and, therefore, it is analytic in the upper half of the complex frequency plane and its real and imaginary parts satisfy Kramers-Kronig relations [77]. As a consequence, we have that ($\tau > 0$)

$$\int_{-\infty}^{\infty}\frac{d\omega}{2\pi}\underline{G}(\mathbf{r}_1,\mathbf{r}_2,\omega)e^{-\mathrm{i}\omega\tau} = \int_{-\infty}^{\infty}\frac{d\omega}{2\pi}\left[\mathrm{P}\int_{-\infty}^{\infty}\frac{d\nu}{\pi}\frac{\underline{G}_I(\mathbf{r}_1,\mathbf{r}_2,\nu)}{\nu-\omega} + \mathrm{i}\underline{G}_I(\mathbf{r}_1,\mathbf{r}_2,\omega)\right]e^{-\mathrm{i}\omega\tau} = 2\mathrm{i}\int_{-\infty}^{\infty}\frac{d\omega}{2\pi}\,\underline{G}_I(\mathbf{r}_1,\mathbf{r}_2,\omega)e^{-\mathrm{i}\omega\tau}. \quad \text{(A2)}$$

In the first line we have used the Kramers-Kronig relations for the real part of the Green tensor, and in the second line we have employed the identity $\mathrm{P}\int_{-\infty}^{\infty}\frac{d\omega}{\pi}\frac{e^{-\mathrm{i}\omega t}}{\nu-\omega} = \mathrm{i}e^{-\mathrm{i}\nu t}$.

In the main text we often encounter the spatial Fourier transform

$$\underline{G}(\mathbf{r}_1,\mathbf{r}_2,\tau) = \int_{-\infty}^{\infty}\frac{d\omega}{2\pi}\int\frac{d^2\mathbf{k}}{(2\pi)^2} \times \underline{G}(\mathbf{k},z,\omega)e^{\mathrm{i}[\mathbf{k}\cdot(\mathbf{R}_1-\mathbf{R}_2)-\omega\tau]}, \quad \text{(A3)}$$

where $\mathbf{k} = (k_x, k_y)$ denotes the in-plane wave vector and the position vectors $\mathbf{r}_1 = (\mathbf{R}_1, z)$ and $\mathbf{r}_2 = (\mathbf{R}_2, z)$ feature the same z-coordinate. From the reality and reciprocity of the Green tensor, one gets $\underline{G}^{\mathsf{T}}(\mathbf{k},z,\omega) = \underline{G}(-\mathbf{k},z;\omega)$, $\underline{G}^*(\mathbf{k},z,\omega) = \underline{G}(-\mathbf{k},z,-\omega)$, and therefore $\underline{G}^\dagger(\mathbf{k},z;\omega) = \underline{G}(\mathbf{k},z,-\omega)$. Based on these properties one can also deduce that the symmetric part of the Green tensor $\underline{G}^{\rm s}(\mathbf{k},z,\omega)$ is even in $\mathbf{k}$, while the antisymmetric part $\underline{G}^{\rm as}(\mathbf{k},z,\omega)$ is odd in $\mathbf{k}$. We can then write

$$\underline{G}_I(\mathbf{r},\mathbf{r}',\omega) = \int\frac{d^2\mathbf{k}}{(2\pi)^2}\,\underline{G}_\Im(\mathbf{k},z,\omega)e^{\mathrm{i}\mathbf{k}\cdot(\mathbf{R}-\mathbf{R}')}, \quad \text{(A4)}$$

where we have defined the tensor

$$\underline{G}_\Im(\mathbf{k},z,\omega) = \frac{\underline{G}(\mathbf{k},z,\omega) - \underline{G}^\dagger(\mathbf{k},z,\omega)}{2\mathrm{i}} = \underline{G}^{\rm s}_I(\mathbf{k},z,\omega) - \mathrm{i}\underline{G}^{\rm as}_R(\mathbf{k},z,\omega). \quad \text{(A5)}$$

As explained in the main text, the total Green tensor can be decomposed as $\underline{G} = \underline{G}_0 + \underline{g}$, where $\underline{G}_0$ is the vacuum contribution and $\underline{g}$ is the scattered part. For a planar surface, we have ($z > 0$)

$$\underline{g}(\mathbf{k},z,\omega) = \frac{\kappa}{2\epsilon_0}\left(r^p[\omega,k]\mathbf{p}_+\mathbf{p}_- + \frac{\omega^2}{c^2\kappa^2}r^s[\omega,k]\mathbf{ss}\right)e^{-2\kappa z}, \quad \text{(A6)}$$

where $\kappa = \sqrt{k^2-\omega^2/c^2}$ ($k = |\mathbf{k}|$, $\mathrm{Re}[\kappa] > 0$ and $\mathrm{Im}[\kappa] < 0$), ϵ_0 is the vacuum permittivity, and $r^\sigma[\omega,k]$ are the polarization dependent ($\sigma = s,p$) reflection coefficients of the surface. Furthermore, in the above expressions, we have defined the polarization vectors [23]

$$\mathbf{s} = \frac{\mathbf{k}}{k}\times\mathbf{z} \quad \mathbf{p}_\pm = \frac{k}{\kappa}\mathbf{z} \mp \mathrm{i}\frac{\mathbf{k}}{k}\ . \quad \text{(A7)}$$

The corresponding dyadic tensors can be written as

$$\mathbf{ss} = \begin{pmatrix} \frac{k_y^2}{k^2} & -\frac{k_y k_x}{k^2} & 0 \\ -\frac{k_y k_x}{k^2} & \frac{k_x^2}{k^2} & 0 \\ 0 & 0 & 0 \end{pmatrix},$$

$$\mathbf{p}_+\mathbf{p}_- = \begin{pmatrix} \frac{k_x^2}{k^2} & \frac{k_y k_x}{k^2} & -\mathrm{i}\frac{k}{\kappa}\frac{k_x}{k} \\ \frac{k_y k_x}{k^2} & \frac{k_y^2}{k^2} & -\mathrm{i}\frac{k}{\kappa}\frac{k_y}{k} \\ \mathrm{i}\frac{k}{\kappa}\frac{k_x}{k} & \mathrm{i}\frac{k}{\kappa}\frac{k_y}{k} & \frac{k^2}{\kappa^2} \end{pmatrix}. \tag{A8}$$

Appendix B: Comparing various expressions for the Casimir-Polder force

Following the procedure described in Section II A, by employing the fluctuation-dissipation theorem one can show that the static Casimir-Polder force can be written as

$$F_{\rm CP} = \frac{\hbar}{\pi}\mathrm{Im}\int_0^\infty d\omega\,\mathrm{Tr}\left[\underline{\alpha}(\omega,\mathbf{r}_a)\cdot\partial_z\underline{G}(\mathbf{r}_a,\mathbf{r},\omega)_{|\mathbf{r}=\mathbf{r}_a}\right]. \tag{B1}$$

Despite formal similarities, Eq. (B1) differs from the standard formulas found in the literature for the atom-surface interaction. Our derivation of Eq. (B1) is different from the expression for the Casimir-Polder force obtained in second-order perturbation theory [1, 23, 24]. In the latter, the position-independent polarizability $\underline{\alpha}^{(0)}(\omega)$ replaces the dressed, position-dependent polarizability $\underline{\alpha}(\omega,\mathbf{r}_a)$ and thus it corresponds to the lowest order of the perturbative expansion of Eq. (B1) in the coupling strength. Indeed, the bare polarizability represents the Fourier transform of the response function $\underline{\alpha}^{(0)}(\tau) = (\mathrm{i}/\hbar)\theta(\tau)\mathrm{tr}[[\hat{\mathbf{d}}^{(0)}(\tau),\hat{\mathbf{d}}^{(0)}(0)]\hat{\rho}_a]$, where only the *free* dipole evolution is considered ($\hat{\rho}_a$ describes the atomic ground state.)

Perhaps more relevant is the difference between Eq. (B1) and the corresponding Lifshitz formula in the scattering formulation [11, 78],

$$F_{\rm CP}^{\rm Lif} = \frac{\hbar}{\pi}\,\mathrm{Im}\int_0^\infty d\omega\mathrm{Tr}\left[\frac{\underline{\alpha}_{\rm vac}(\omega)\cdot\partial_z\underline{g}(\mathbf{r}_a,\mathbf{r},\omega)}{1-\underline{\alpha}_{\rm vac}(\omega)\cdot\underline{g}(\mathbf{r}_a,\mathbf{r},\omega)}\right]_{|\mathbf{r}=\mathbf{r}_a}. \tag{B2}$$

In this case, the force is given in terms of the scattering properties of the surface and the atom is treated as a non-interacting scatterer: The quantity $\underline{\alpha}_{\rm vac}(\omega)$ is the position-independent dressed polarizability for the atom placed in the free electromagnetic vacuum (it differs from $\underline{\alpha}^{(0)}(\omega)$ as it contains the Lamb shift and spontaneous decay rate), while $\underline{g}(\mathbf{r},\mathbf{r}',\omega)$ is again the scattered part of the Green tensor [11]. The denominator in the above expression indicates multiple reflections of the electric field between the atom and the surface. Keeping only one round-trip in the atom-surface multiple reflections process [79], one obtains an expression which is formally similar to Eq.(B1) but where $\underline{\alpha}_{\rm vac}(\omega)$ replaces $\underline{\alpha}(\omega,\mathbf{r}_a)$.

When all multiple reflections are kept, Eq. (B2) becomes identical to Eq.(B1) provided that

$$\underline{\alpha}(\mathbf{r}_a,\omega) = \left[1-\underline{\alpha}_{\rm vac}(\omega)\cdot\underline{g}(\mathbf{r}_a,\mathbf{r}_a,\omega)\right]^{-1}\cdot\alpha_{\rm vac}(\omega). \tag{B3}$$

This corresponds to a re-summation of the perturbation series, and the underlying condition is that the atom responds linearly to the electric field (and the higher multipoles can be neglected). For example, when the atom is modeled as a linear harmonic oscillator, the equation of motion of the dipole operator $\hat{\mathbf{d}} = \mathbf{d}\hat{q}$ is

$$\ddot{\hat{q}}(t) + \omega_a^2\hat{q}(t) = \frac{2\omega_a}{\hbar}\mathbf{d}\cdot\hat{\mathbf{E}}(\mathbf{r}_a,t)\,. \tag{B4}$$

Here, $\hat{\mathbf{E}}(\mathbf{r},t) = \hat{\mathbf{E}}_0(\mathbf{r},t) + \hat{\mathbf{E}}_{\rm S}(\mathbf{r},t)$ is the sum of the field without the atom ($\mathbf{E}_0(\mathbf{r},t)$) and the radiation reaction field ($\mathbf{E}_{\rm S}(\mathbf{r},\omega) = \underline{G}(\mathbf{r},\mathbf{r}_a,\omega)\cdot\mathbf{d}\hat{q}(\omega)$). In Fourier space, the stationary dipole's dynamics is then given by $\hat{\mathbf{d}}(\omega,\mathbf{r}_a) = \underline{\alpha}(\omega,\mathbf{r}_a)\cdot\hat{\mathbf{E}}_0(\mathbf{r}_a,\omega)$ which implicitly defines the atom's polarizability as

$$\underline{\alpha}(\mathbf{r}_a,\omega) = \frac{\frac{2\omega_a}{\hbar}\mathbf{dd}}{\omega_a^2-\omega^2-\frac{2\omega_a}{\hbar}\mathbf{d}\cdot\underline{G}(\mathbf{r}_a,\mathbf{r}_a,\omega)\cdot\mathbf{d}}. \tag{B5}$$

This is the expression for the polarizability that enters in Eq.(B1) which, as expected, depends on the position of the oscillator through the Green tensor. If the atom is isolated in vacuum, one must replace $\underline{G}$ by $\underline{G}_0$ to recover $\alpha_{\rm vac}(\omega)$. Finally, using that $\underline{G} = \underline{G}_0 + \underline{g}$ one can show that, in the case Eq. (B5), $\underline{\alpha}(\mathbf{r}_a,\omega)$ and $\alpha_{\rm vac}(\omega)$ are related as described in Eq. (B3).

Appendix C: The quantum regression theorem

We provide here the main steps that lead to the result known as the quantum regression theorem [25]. We will consider the time evolutions of quantities related to a coupled quantum system given by a small subsystem "S" and a large stationary environment (reservoir) "R", which for simplicity is also assumed to be in thermal equilibrium. The eigenvectors $|E_n\rangle$ of the Hamiltonian $\hat{H}_S$ describing the free evolution of the system "S" are chosen as basis of the corresponding Hilbert space. The total system is described at the time t by the density matrix $\hat{\rho}(t)$.

Consider the function $C_B^{nm}(t,\tau) = \mathrm{tr}[\hat{A}_{mn}(t+\tau)\hat{B}(t)\hat{\rho}(0)]$ ($\tau > 0$) where $\hat{A}_{mn} = |E_m\rangle\langle E_n|$ and $\hat{B}$ is a generic operator having support only on the Hilbert space of "S". We have that $C_B^{nm}(t,\tau) = \mathrm{tr}_S[\hat{A}_{mn}\hat{\chi}_S^B(\tau;t)]$ where we have defined

$$\hat{\chi}_S^B(\tau;t) = \mathrm{tr}_R[e^{-\frac{\mathrm{i}}{\hbar}\hat{H}\tau}\hat{\chi}^B(0;t)e^{\frac{\mathrm{i}}{\hbar}\hat{H}\tau}]\,, \tag{C1}$$

where the symbol $\mathrm{tr}_{R(S)}$ indicates the trace only of the reservoir's (subsystem's) quantum degrees of freedom. If we look at $\hat{\chi}^B(0;t) = \hat{B}\hat{\rho}(t)$ as a the initial condition for

a density matrix, $\hat{\chi}_S^B(\tau;t)$ is the time evolution in τ of the reduced density matrix obtained after the trace over the reservoir. Using the Born approximation and the theory of open quantum system [4, 5] we can derive in general that

$$\partial_\tau \hat{\chi}_S^B(\tau;t) = \left[-\frac{\mathrm{i}}{\hbar}\mathcal{H}_S - \mathcal{L}(\tau)\right]\hat{\chi}_S^B(\tau;t)\ , \tag{C2}$$

where the superoperator $\mathcal{H}_S = [\hat{H}_S, \cdot]$ describes the free evolution of the subsystem, while $\mathcal{L}(\tau)$ is a superoperator related to the interaction with the environment. The previous equation requires only that the initial density matrix is factorized

$$\hat{\chi}^B(0;t) = \hat{B}\hat{\rho}(t) \approx \hat{B}\hat{\rho}_S(t)\otimes\hat{\rho}_R = \hat{\chi}_S^B(0;t)\otimes\hat{\rho}_R\ , \tag{C3}$$

which can be seen as a consequence of the Born approximation. The density matrix $\hat{\rho}_S(t)$ is the reduced density matrix of the subsystem, while $\hat{\rho}_R$ describes the state of the environment, which will be assumed to be stationary. The superoperator $\mathcal{L}(\tau)$ can expressed as an infinite series using the time-convolutionless (TCL) approach [5, 80–82] or equivalently as an integral operator involving a memory kernel $\mathcal{K}(\tau')$, i.e.

$$\mathcal{L}(\tau)\hat{\chi}_S^B(\tau;t) \equiv \int_0^\tau d\tau' \mathcal{K}(\tau')\hat{\chi}_S^B(\tau-\tau';t)\ . \tag{C4}$$

Within the Markov approximation $\mathcal{L}(\tau)\hat{\chi}_S^B(\tau;t) \to \mathcal{L}\hat{\chi}_S^B(\tau;t)$ and the superoperator $\mathcal{L} = \int_0^\infty d\tau'\mathcal{K}(\tau')$ becomes time independent and is no longer a convolution. Since $\hat{\chi}_S^B(\tau;t)$ has support on the Hilbert space "S", using the expansion $\hat{\chi}_S^B(\tau;t) = \sum_{ij}\mathrm{tr}_S[\hat{A}_{ij}^\dagger\hat{\chi}_S^B(\tau;t)]\hat{A}_{ij}$ we obtain

$$\begin{aligned}\partial_\tau C_B^{nm}(t,\tau) &= \mathrm{tr}_S[\hat{A}_{mn}\left[-\frac{\mathrm{i}}{\hbar}\mathcal{H}_S - \mathcal{L}(\tau)\right]\hat{\chi}_S^B(\tau;t)] \\ &= \sum_{ij}\mathrm{tr}_S[\hat{A}_{mn}\left[-\frac{\mathrm{i}}{\hbar}\mathcal{H}_S - \mathcal{L}(\tau)\right]\hat{A}_{ij}]\mathrm{tr}_S[\hat{A}_{ij}^\dagger\hat{\chi}_S^B(\tau;t)] \\ &= \sum_{ij}\left[-\mathrm{i}\omega_{ij}\delta_{ij}^{nm} - \mathcal{L}_{ij}^{nm}(\tau)\right]C_B^{ij}(t,\tau)\end{aligned} \tag{C5}$$

($\delta_{ij}^{nm} = \delta_{ni}\delta_{mj}$ and $\mathcal{L}_{ij}^{nm}(\tau) = \mathrm{tr}_S[\hat{A}_{nm}^\dagger\mathcal{L}(\tau)\hat{A}_{ij}]$) which is Eq.(11). In the previous expression we used that $\mathcal{L}(\tau)$ is a linear superoperator to take out the sum symbol (this does not mean that the systems dynamics is linear).

Appendix D: Using the QRT for calculating the Casimir-Polder force

Within the QRT approach, the Casimir-Polder force is given as an integration over real frequencies via equation (13). It can be decomposed into four terms

$$F_{\mathrm{CP}}^{\mathrm{QRT}} = \int_0^\infty \frac{d\omega}{2\pi\mathrm{i}}\frac{\mathrm{Tr}\left[\mathbf{dd}\cdot\partial_z\underline{G}(\mathbf{r}_a,\mathbf{r},\omega)_{|\mathbf{r}=\mathbf{r}_a}\right]}{\omega+\tilde{\omega}_a(\mathbf{r}_a)-\mathrm{i}\gamma(\mathbf{r}_a)} \tag{D1a}$$

$$-\int_0^\infty \frac{d\omega}{2\pi\mathrm{i}}\frac{\mathrm{Tr}\left[\mathbf{dd}\cdot\partial_z\underline{G}^*(\mathbf{r}_a,\mathbf{r},\omega)_{|\mathbf{r}=\mathbf{r}_a}\right]}{\omega+\tilde{\omega}_a(\mathbf{r}_a)-\mathrm{i}\gamma(\mathbf{r}_a)} \tag{D1b}$$

$$+\int_0^\infty \frac{d\omega}{2\pi\mathrm{i}}\frac{\mathrm{Tr}\left[\mathbf{dd}\cdot\partial_z\underline{G}(\mathbf{r}_a,\mathbf{r},\omega)_{|\mathbf{r}=\mathbf{r}_a}\right]}{\omega+\tilde{\omega}_a(\mathbf{r}_a)+\mathrm{i}\gamma(\mathbf{r}_a)} \tag{D1c}$$

$$-\int_0^\infty \frac{d\omega}{2\pi\mathrm{i}}\frac{\mathrm{Tr}\left[\mathbf{dd}\cdot\partial_z\underline{G}^*(\mathbf{r}_a,\mathbf{r},\omega)_{|\mathbf{r}=\mathbf{r}_a}\right]}{\omega+\tilde{\omega}_a(\mathbf{r}_a)+\mathrm{i}\gamma(\mathbf{r}_a)}, \tag{D1d}$$

where $\tilde{\omega}_a(\mathbf{r}_a)$ and $\gamma(\mathbf{r}_a)$ are non-negative quantities. The integrand in (D1c) has poles in the lower part of the complex-frequency plane. Thus, a standard Wick rotation can be performed, resulting in an integration over the positive imaginary frequency axis. For the integral in (D1a), we notice that the integrand has all poles in the lower part of the complex-frequency plane with the exception of $\omega = -\tilde{\omega}_a(\mathbf{r}_a)+\mathrm{i}\gamma(\mathbf{r}_a)$ which is actually located in the upper left quadrant. This means that a similar Wick rotation in the first integrand is still possible. For the term appearing in (D1b) we can utilize that $\underline{G}^*(\mathbf{r}_a,\mathbf{r},\omega) = \underline{G}(\mathbf{r}_a,\mathbf{r},-\omega)$ and a change of variable $\omega\to-\omega$. The resulting integral running from $-\infty$ to zero concerns an integrand with poles in the lower part of the complex-frequency plane. A similar procedure for the term in (D1d) leads to an integral where all the poles of the Green tensor are in the lower part of the complex-frequency plane, except for one pole at $\omega = \tilde{\omega}_a(\mathbf{r}_a)+\mathrm{i}\gamma(\mathbf{r}_a)$ that is located in the first quadrant. Since the corresponding integral again runs from $-\infty$ to zero we can still perform a rotation of the complex path in the second quadrant. This procedure leads to

$$\begin{aligned}F_{\mathrm{CP}}^{\mathrm{QRT}} = &\int_0^\infty \frac{d\xi}{2\pi}\frac{\mathrm{Tr}\left[\mathbf{dd}\cdot\partial_z\underline{G}(\mathbf{r}_a,\mathbf{r},\mathrm{i}\xi)_{|\mathbf{r}=\mathbf{r}_a}\right]}{\tilde{\omega}_a(\mathbf{r}_a)-(-\mathrm{i}\xi+\mathrm{i}\gamma(\mathbf{r}_a))} \\ &+\int_0^\infty \frac{d\xi}{2\pi}\frac{\mathrm{Tr}\left[\mathbf{dd}\cdot\partial_z\underline{G}(\mathbf{r}_a,\mathbf{r},\mathrm{i}\xi)_{|\mathbf{r}=\mathbf{r}_a}\right]}{\tilde{\omega}_a(\mathbf{r}_a)-(\mathrm{i}\xi+\mathrm{i}\gamma(\mathbf{r}_a))} \\ &+\int_0^\infty \frac{d\xi}{2\pi}\frac{\mathrm{Tr}\left[\mathbf{dd}\cdot\partial_z\underline{G}(\mathbf{r}_a,\mathbf{r},\mathrm{i}\xi)_{|\mathbf{r}=\mathbf{r}_a}\right]}{\tilde{\omega}_a(\mathbf{r}_a)+(\mathrm{i}\xi+\mathrm{i}\gamma(\mathbf{r}_a))} \\ &+\int_0^\infty \frac{d\xi}{2\pi}\frac{\mathrm{Tr}\left[\mathbf{dd}\cdot\partial_z\underline{G}(\mathbf{r}_a,\mathbf{r},\mathrm{i}\xi)_{|\mathbf{r}=\mathbf{r}_a}\right]}{\tilde{\omega}_a(\mathbf{r}_a)+(-\mathrm{i}\xi+\mathrm{i}\gamma(\mathbf{r}_a))}.\end{aligned} \tag{D2}$$

Equation (14) is then recovered from Eq. (D2) by using the definition in Eq.(15).

It is also interesting to show that the non-Markovian contribution in Eq. (16) is directly responsible for the difference between the result of the QRT in Eq. (14) and Eq. (10) obtained via the FDT. Upon inserting the second term on the right-hand side of Eq. (16) into the

expression of the Casimir-Polder force Eq. (4), we have

$$\begin{aligned} F_{\rm CP}^{\rm nM} &= {\rm Re}\Big(\frac{2}{\pi}\int_0^\infty d\omega \int_0^\infty d\tau e^{-{\rm i}\omega\tau} \\ &\quad \times {\rm Tr}\Big[\Big\{\frac{\hbar}{\pi}\int_0^\infty d\xi e^{-\xi\tau}[\underline{\alpha}_I(\omega)]_{|\omega=-{\rm i}\xi+0^+}\Big\} \\ &\quad \cdot \partial_z \underline{G}_I(\mathbf{r}_a,\mathbf{r},\omega)_{|\mathbf{r}=\mathbf{r}_a}\Big]\Big) \\ &= {\rm Tr}\Big[\frac{\hbar}{\pi}\int_0^\infty d\xi \frac{\underline{\alpha}({\rm i}\xi)-\underline{\alpha}(-{\rm i}\xi)}{2} \\ &\quad \cdot \frac{2}{\pi}\int_0^\infty d\omega \,\frac{\omega\partial_z \underline{G}_I(\mathbf{r}_a,\mathbf{r},\omega)_{|\mathbf{r}=\mathbf{r}_a}}{\omega^2+\xi^2}\Big] \\ &= \frac{\hbar}{\pi}\int_0^\infty d\xi {\rm Tr}\Big[\frac{\underline{\alpha}({\rm i}\xi)-\underline{\alpha}(-{\rm i}\xi)}{2} \\ &\quad \cdot \partial_z \underline{G}(\mathbf{r}_a,\mathbf{r},{\rm i}\xi)_{|\mathbf{r}=\mathbf{r}_a}\Big], \end{aligned} \tag{D3}$$

where we have already assumed that the polarization tensor is symmetric (see Eq.(15)). In addition, in the last step we have used the Kramers-Kronig relation (for simplicity, we have suppressed the dependence of the polarizability on $\mathbf{r}_a$). When added to Eq. (14) the above expression reproduces Eq. (10).

Appendix E: Non-Markovian contribution to quantum friction

The importance of non-Markovianity in quantum friction can be assessed by considering the term $\underline{S}_{\rm nM}(\mathbf{k}\cdot\mathbf{v}-\omega)$ defined in Eq. (30). Using Eqs. (23) and (30) we obtain (for simplicity we consider $\mathbf{v}=v_x\mathbf{x}$)

$$\begin{aligned} F_{\rm fric}^{\rm nM} &= \frac{2\hbar}{\pi}\int \frac{d^2\mathbf{k}}{(2\pi)^2}k_x \int_{k_x v_x}^\infty d\omega \\ &\quad \times {\rm Tr}\left[{\rm Re}\sum_\mu \frac{{\rm iRes}[\underline{\alpha}(\Omega_\mu)]}{\Omega_\mu+\omega-k_x v_x}\cdot \underline{G}_I^{\rm s}(\mathbf{k},z_a,\omega)\right] \\ &\quad + \frac{2\hbar}{\pi}\int \frac{d^2\mathbf{k}}{(2\pi)^2}k_x \int_0^{k_x v_x} d\omega \\ &\quad \times {\rm Tr}\left[{\rm Re}\sum_\mu \frac{{\rm iRes}[\underline{\alpha}(\Omega_\mu)]}{\Omega_\mu+k_x v_x-\omega}\cdot \underline{G}_I^{\rm s}(\mathbf{k},z_a,\omega)\right]. \end{aligned} \tag{E1}$$

Recalling that $\underline{G}_I^{\rm s}(\mathbf{k},z_a,\omega=0)=0$, the leading term in the expansion for low velocities is provided by the first term on the right-hand side of this equation. Consequently, we obtain to leading order

$$\begin{aligned} F_{\rm fric}^{\rm nM} &\approx \frac{2\hbar v_x}{\pi}\int \frac{d^2\mathbf{k}}{(2\pi)^2}k_x^2 \int_0^\infty d\omega \\ &\quad \times {\rm Tr}\left[{\rm Re}\sum_\mu \frac{{\rm iRes}[\underline{\alpha}(\Omega_\mu)]}{(\Omega_\mu+\omega)^2}\cdot \underline{G}_I^{\rm s}(\mathbf{k},z_a,\omega)\right]. \end{aligned} \tag{E2}$$

This exactly compensates the contribution arising from the QRT (cfr. Eq. (32)).

[1] H. B. G. Casimir and D. Polder, *The Influence of Retardation on the London-van der Waals Forces*, Phys. Rev. **73**, 360 (1948).

[2] J. B. Pendry, *Shearing the vacuum - quantum friction*, J. Phys.: Condes. Matter **9**, 10301 (1997).

[3] A. I. Volokitin and B. N. J. Persson, *Near-field radiative heat transfer and noncontact friction*, Rev. Mod. Phys. **79**, 1291 (2007).

[4] C. Gardiner, *Quantum Noise* (Springer-Verlag, Berlin, 1991).

[5] H. Breuer and F. Petruccione, *The Theory of Open Quantum Systems* (Oxford University Press, Oxford, 2002).

[6] Á. Rivas, S. F. Huelga, and M. B. Plenio, *Quantum non-Markovianity: characterization, quantification and detection*, Reports on Progress in Physics **77**, 094001 (2014).

[7] H.-P. Breuer, E.-M. Laine, J. Piilo, and B. Vacchini, *Colloquium : Non-Markovian dynamics in open quantum systems*, Rev. Mod. Phys. **88**, 021002 (2016).

[8] H.-P. Breuer, E.-M. Laine, and J. Piilo, *Measure for the Degree of Non-Markovian Behavior of Quantum Processes in Open Systems*, Phys. Rev. Lett. **103**, 210401 (2009).

[9] Á. Rivas, S. F. Huelga, and M. B. Plenio, *Entanglement and Non-Markovianity of Quantum Evolutions*, Phys. Rev. Lett. **105**, 050403 (2010).

[10] U. Hoeppe, C. Wolff, J. Küchenmeister, J. Niegemann, M. Drescher, H. Benner, and K. Busch, *Direct Observation of Non-Markovian Radiation Dynamics in 3D Bulk Photonic Crystals*, Phys. Rev. Lett. **108**, 043603 (2012).

[11] F. Intravaia, C. Henkel, and M. Antezza, in *Casimir Physics*, Vol. 834 of *Lecture Notes in Physics*, edited by D. Dalvit, P. Milonni, D. Roberts, and F. da Rosa (Springer, Berlin / Heidelberg, 2011), pp. 345–391.

[12] S. Y. Buhmann, L. Knoell, D.-G. Welsch, and H. T. Dung, *Casimir-Polder forces: A nonperturbative approach*, Phys. Rev. A **70**, 052117 (2004).

[13] I. E. Dzyaloshinskii, E. M. Lifshitz, and L. P. Pitaevskii, *General Theory of the van der Waals' Forces*, Sov. Phys. Usp. **4**, 153 (1961).

[14] P. W. Milonni, J. R. Ackerhalt, and W. A. Smith, *Interpretation of Radiative Corrections in Spontaneous Emission*, Phys. Rev. Lett. **31**, 958 (1973).

[15] J. Dalibard, J. Dupont-Roc, and C. Cohen-Tannoudji, *Vacuum fluctuations and radiation reaction : identification of their respective contributions*, J. Phys. France **43**, 1617 (1982).

[16] G. W. Ford and R. F. O'Connell, *A Quantum Violation of the Second Law?*, Phys. Rev. Lett. **96**, 020402 (2006).

[17] F. Intravaia and C. Henkel, *Casimir energy and entropy between dissipative mirrors*, J. Phys. A: Math. Gen. **41**, 164018 (9pp) (2008).

[18] G. Compagno, R. Passante, and F. Persico, *Atom-field interactions and dressed atoms* (Cambridge University Press, Cambridge, UK, 2005), Vol. 17.

[19] R. Kubo, *Statistical-Mechanical Theory of Irreversible Processes. I. General Theory and Simple Applications to Magnetic and Conduction Problems*, J. Phys. Soc. Jap. **12**, 570 (1957).

[20] R. Kubo, *The fluctuation-dissipation theorem*, Rep. Prog. Phys. **29**, 255 (1966).

[21] R. Haag, N. Hugenholtz, and M. Winnink, *On the equilibrium states in quantum statistical mechanics*, Comm. Math. Phys. **5**, 215 (1967).

[22] H. B. Callen and T. A. Welton, *Irreversibility and Generalized Noise*, Phys. Rev. **83**, 34 (1951).

[23] J. M. Wylie and J. E. Sipe, *Quantum electrodynamics near an interface*, Phys. Rev. A **30**, 1185 (1984).

[24] A. D. McLachlan, *Retarded Dispersion Forces in Dielectrics at Finite Temperatures*, Proc. R. Soc. Lond. A **274**, 80 (1963).

[25] M. Lax, *Formal Theory of Quantum Fluctuations from a Driven State*, Phys. Rev. **129**, 2342 (1963).

[26] L. Mandel and E. Wolf, *Optical Coherence and Quantum Optics* (Cambridge University Press, New York, 1995).

[27] L. Onsager, *Reciprocal Relations in Irreversible Processes. I.*, Phys. Rev. **37**, 405 (1931).

[28] L. Onsager, *Reciprocal Relations in Irreversible Processes. II.*, Phys. Rev. **38**, 2265 (1931).

[29] N. G. Van Kampen, *Stochastic processes in physics and chemistry*, third edition ed. (Elsevier, Amsterdam, 1992), Vol. 1.

[30] It is important to point out, however, that this is only an approximation valid in weak coupling. In reality, if thermalization occurs, it is the global system that goes to a highly correlated stationary equilibrium state; the reduced state of the total coupled system is given by a mixture of ground and excited states and although the mean value can become constant, its value can be different from that it would take in the ground state of the subsystem.

[31] P. Talkner, *The failure of the quantum regression hypothesis*, Ann. Phys. **167**, 390 (1986).

[32] G. W. Ford and R. F. O'Connell, *There is No Quantum Regression Theorem*, Phys. Rev. Lett. **77**, 798 (1996).

[33] G. Ford and R. O'Connell, *Driven systems and the Lax formula*, Opt. Comm. **179**, 451 (2000).

[34] M. Lax, *The Lax-Onsager regression 'theorem' revisited*, Opt. Comm. **179**, 463 (2000).

[35] G. Ford and R. O'Connell, *Comment on The Lax-Onsager Regression Theorem revisited*, Opt. Comm. **179**, 477 (2000).

[36] L. Allen and J. H. Eberly, *Optical resonance and two-level atoms* (Dover, New York, 1975).

[37] Our approach parallels closely Ref.[12] where also a generalization to multi-level atoms can be found. In the multi-level case, further approximations beyond the Born-Markov are often performed at the level of the master-equation for the mean values to neglect the couplings between different off-diagonal transitions and between off-diagonal and diagonal transitions.

[38] P. W. Milonni and R. W. Boyd, *Influence of radiative damping on the optical-frequency susceptibility*, Phys. Rev. A **69**, 023814 (2004).

[39] G. Lach, M. DeKieviet, and U. D. Jentschura, *Enhancement of Blackbody Friction due to the Finite Lifetime of Atomic Levels*, Phys. Rev. Lett. **108**, 043005 (2012).

[40] D. Jentschura, U., G. Lach, M. De Kieviet, and K. Pachucki, *One-Loop Dominance in the Imaginary Part of the Polarizability: Application to Blackbody and Noncontact van der Waals Friction*, Phys. Rev. Lett. **114**, 043001 (2015).

[41] S. Y. Buhmann, S. Scheel, S. Å. Ellingsen, K. Hornberger, and A. Jacob, *Casimir-Polder interaction of fullerene molecules with surfaces*, Phys. Rev. A **85**, 042513 (2012).

[42] D. A. Steck, Technical report, Oregon Center for Optics and Department of Physics, University of Oregon.

[43] G. Guarnieri, A. Smirne, and B. Vacchini, *Quantum regression theorem and non-Markovianity of quantum dynamics*, Phys. Rev. A **90**, 022110 (2014).

[44] N. L. Gullo, I. Sinayskiy, T. Busch, and F. Petruccione, *Non-Markovianity criteria for open system dynamics*, arXiv preprint arXiv:1401.1126 (2014).

[45] M. M. Ali, P.-Y. Lo, M. W.-Y. Tu, and W.-M. Zhang, *Non-Markovianity measure using two-time correlation functions*, Phys. Rev. A **92**, 062306 (2015).

[46] P. L. Knight and P. W. Milonni, *Long-time deviations from exponential decay in atomic spontaneous emission theory*, Phys. Lett. A **56**, 275 (1976).

[47] P. R. Berman and G. W. Ford, in *Advances In Atomic, Molecular, and Optical Physics*, edited by E. Arimondo, P. R. Berman, and C. C. Lin (Academic Press, Amsterdam, 2010), Vol. 59, p. 175.

[48] R. Davidson and J. J. Kozak, *On the Relaxation to Quantum-Statistical Equilibrium of the Wigner-Weisskopf Atom in a One-Dimensional Radiation Field. I. A Study of Spontaneous Emission*, J. Math. Phys. **11**, 189 (1970).

[49] R. Davidson and J. J. Kozak, *Relaxation to Quantum-Statistical Equilibrium of the Wigner-Weisskopf Atom in a One-Dimensional Radiation Field. III. The Quantum-Mechanical Solution*, J. Math. Phys. **12**, 903 (1971).

[50] K. Wódkiewicz and J. H. Eberly, *Markovian and nonmarkovian behavior in two-level atom fluorescence*, Ann. Phys. **101**, 574 (1976).

[51] V. Weisskopf and E. Wigner, *Berechnung der natürlichen Linienbreite auf Grund der Diracschen Lichttheorie*, Z. Physik **63**, 54 (1930).

[52] T. von Foerster, *Quantum Theory of a Damped Two-Level Atom*, Am. J. Phys. **40**, 854 (1972).

[53] C. Cohen-Tannoudji, J. Dupont-Roc, and G. Grynberg, *Atom-photon interactions* (John Wiley and Sons Inc., New York, 1998).

[54] G. Dedkov and A. Kyasov, *Electromagnetic and fluctuation-electromagnetic forces of interaction of moving particles and nanoprobes with surfaces: A nonrelativistic consideration*, Phys. Solid State **44**, 1809 (2002).

[55] G. Barton, *On van der Waals friction. II: Between atom and half-space*, New J. Phys. **12**, 113045 (2010).

[56] F. Intravaia, V. E. Mkrtchian, S. Y. Buhmann, S. Scheel, D. A. R. Dalvit, and C. Henkel, *Friction forces on atoms after acceleration*, J. Phys.: Condes. Matter **27**, 214020 (2015).

[57] S. Scheel and S. Y. Buhmann, *Casimir-Polder forces on moving atoms*, Phys. Rev. A **80**, 042902 (2009).

[58] F. Intravaia, R. O. Behunin, C. Henkel, K. Busch, and

D. A. R. Dalvit, *Failure of Local Thermal Equilibrium in Quantum Friction*, Phys. Rev. Lett. **117**, 100402 (2016).
[59] M. F. Maghrebi, R. L. Jaffe, and M. Kardar, *Spontaneous Emission by Rotating Objects: A Scattering Approach*, Phys. Rev. Lett. **108**, 230403 (2012).
[60] M. F. Maghrebi, R. Golestanian, and M. Kardar, *Quantum Cherenkov radiation and noncontact friction*, Phys. Rev. A **88**, 042509 (2013).
[61] J. S. Høye and I. Brevik, *Casimir friction at zero and finite temperatures*, Eur. Phys. J. D **68**, 1 (2014).
[62] D. Polder and M. Van Hove, *Theory of Radiative Heat Transfer between Closely Spaced Bodies*, Phys. Rev. B **4**, 3303 (1971).
[63] J. M. Obrecht, R. J. Wild, M. Antezza, L. P. Pitaevskii, S. Stringari, and E. A. Cornell, *Measurement of the Temperature Dependence of the Casimir-Polder Force*, Phys. Rev. Lett. **98**, 063201 (2007).
[64] F. Intravaia, R. O. Behunin, and D. A. R. Dalvit, *Quantum friction and fluctuation theorems*, Phys. Rev. A **89**, 050101(R) (2014).
[65] V. Frolov and V. Ginzburg, *Excitation and radiation of an accelerated detector and anomalous Doppler effect*, Phys. Lett. A **116**, 423 (1986).
[66] V. L. Ginzburg, *Radiation by uniformly moving sources (Vavilov–Cherenkov effect, transition radiation, and other phenomena)*, Physics-Uspekhi **39**, 973 (1996).
[67] P. A. Čerenkov, *Visible Radiation Produced by Electrons Moving in a Medium with Velocities Exceeding that of Light*, Phys. Rev. **52**, 378 (1937).
[68] I. Frank and I. Tamm, *Coherent visible radiation of fast electrons passing through matter*, C.R. Acad. Sci. URSS **14**, 109 (1937).
[69] S. I. Maslovski and M. G. Silveirinha, *Casimir forces at the threshold of the Cherenkov effect*, Phys. Rev. A **84**, 062509 (2011).
[70] G. Pieplow and C. Henkel, *Cherenkov friction on a neutral particle moving parallel to a dielectric*, J. Phys.: Condes. Matter **27**, 214001 (2015).
[71] J. Klatt, R. Bennett, and S. Y. Buhmann, eprint: arXiv:1601.02765.
[72] G. Pieplow and C. Henkel, *Fully covariant radiation force on a polarizable particle*, New J. Phys. **15**, 023027 (2013).
[73] G. Dedkov and A. Kyasov, *The relativistic theory of fluctuation electromagnetic interactions of moving neutral particles with a flat surface*, Phys. Solid State **45**, 1815 (2003).
[74] A. I. Volokitin and B. N. J. Persson, *Theory of the interaction forces and the radiative heat transfer between moving bodies*, Phys. Rev. B **78**, 155437 (2008).
[75] M. G. Silveirinha, *Optical Instabilities and Spontaneous Light Emission by Polarizable Moving Matter*, Phys. Rev. X **4**, 031013 (2014).
[76] It is interesting to notice that, in agreement with Eq. (29), a calculation at the fourth order in the dipole strength for systems with induced dissipation shows a low-velocity asymptotic behavior which is very similar to that described in Eq. (39). The main difference is that γ is essentially replaced by the low-frequency expression of the position-dependent radiative decay rate [58, 64]. This also indicates that, in such systems the functional dependence of quantum friction on the atom-surface distance is modified relative to that of systems with intrinsic dissipation [55, 57, 64].
[77] J. Jackson, *Classical Electrodynamics* (John Wiley and Sons Inc., New York, 1975).
[78] F. Intravaia and R. Behunin, *Casimir effect as a sum over modes in dissipative systems*, Phys. Rev. A **86**, 062517 (2012).
[79] R. Messina, D. A. R. Dalvit, P. A. Maia Neto, A. Lambrecht, and S. Reynaud, *Dispersive interactions between atoms and nonplanar surfaces*, Phys. Rev. A **80**, 022119 (2009).
[80] S. Nakajima, *On Quantum Theory of Transport Phenomena: Steady Diffusion*, Prog. Theor. Phys. **20**, 948 (1958).
[81] R. Zwanzig, *Ensemble Method in the Theory of Irreversibility*, The Journal of Chemical Physics **33**, 1338 (1960).
[82] R. Zwanzig, *On the identity of three generalized master equations*, Physica **30**, 1109 (1964).
[83] J. Gieseler, R. Quidant, C. Dellago, and L. Novotny, *Dynamic relaxation of a levitated nanoparticle from a non-equilibrium steady state*, Nature Nanotech. **9**, 358 (2014).
[84] V. Jain, J. Gieseler, C. Moritz, C. Dellago, R. Quidant, and L. Novotny, *Direct Measurement of Photon Recoil from a Levitated Nanoparticle*, Phys. Rev. Lett. **116**, 243601 (2016).
[85] A. Laliotis, T. P. de Silans, I. Maurin, M. Ducloy, and D. Bloch, *Casimir-Polder interactions in the presence of thermally excited surface modes*, Nature Comm. **5**, (2014).
[86] K. Hornberger, S. Gerlich, P. Haslinger, S. Nimmrichter, and M. Arndt, *Colloquium : Quantum interference of clusters and molecules*, Rev. Mod. Phys. **84**, 157 (2012).
[87] F. Impens, R. O. Behunin, C. C. Ttira, and P. A. M. Neto, *Non-local double-path Casimir phase in atom interferometers*, Europhys. Lett. **101**, 60006 (2013).